NASA

National Aeronautics and
Space Administration

DESIGN OF A V/STOL PROPULSION SYSTEM FOR A LARGE-SCALE FIGHTER MODEL

FINAL REPORT

MAY 1981

by

W.S. Willis

GENERAL ELECTRIC COMPANY

Prepared For

National Aeronautics and Space Administration

NASA-Ames Research Center
Contract No. NAS2-10156

TABLE OF CONTENTS

LIST OF ILLUSTRATIONS

LIST OF ILLUSTRATIONS (Concluded)

LIST OF TABLES

1.0 SUMMARY

This report covers a study conducted by the General Electric Company of modifications to the existing large-scale STOL fighter model needed to simulate a V/STOL configuration. The modifications consist of adding two-dimensional lift/cruise exhaust nozzles to the existing nacelle-mounted J97 engines and adding a third fuselage-mounted J97 engine to supply exhaust gas to a simulated remote augmented lift system (RALS) exhaust nozzle in the forward fuselage.

The study included a determination of the requirements and RALS propulsion system operating conditions, an evaluation of the J97 engine capability to simulate the gas flow to a remote exhaust nozzle, the development of the required inlet and exhaust duct flowpaths, the detailed design and mechanical analysis of the hot ducting to the remote nozzle, and the layout of a two-dimensional lift/cruise exhaust nozzle for use on the nacelle-mounted J97 engines.

The study resulted in sufficient design information to ensure that there are no mechanical or aerodynamic design limitations that would interfere with the intended testing of the model. An inlet distortion analysis was conducted providing guidance to the rate of throttle movements allowable and a recommendation of the inlet instrumentation needed to ensure against stalling the third J97 engine. A detailed design of the hot ducting and remote exhaust nozzle defined nonflightweight hardware suitable for fabrication at ARC.

2.0 INTRODUCTION

A large-scale STOL fighter model (Figure 1) has been fabricated and tested in the ARC 40- by 80-Foot Wind Tunnel. This model is a part of a program to develop a highly maneuverable supersonic fighter. Testing has been completed of a configuration powered by two nacelle-mounted J97 engines. Next, it is desired to modify the model to simulate a V/STOL configuration.

The RALS concept has been proposed to General Electric as a means to supply a controllable forward lift vector in a V/STOL aircraft. The concept has been evaluated under contracts from the Naval Air Propulsion Center (References 1, 2, 3, and 4). These studies showed that compared to propulsion systems using dedicated lift engines the RALS system can provide about the same size (TOGW) supersonic fighter aircraft to complete the specified deck-launched intercept mission. However, since all of the installed turbomachinery is available to provide forward thrust, the RALS-powered aircraft far exceeds concepts using dedicated lift engines in terms of supersonic acceleration and combat specific energy, P_s.

Recent USAF emphasis has been placed on the need for a land-based fighter that meets the stringent requirements of runway denial. Although not envisioned as requiring pure vertical takeoff, this aircraft would require very short takeoff capability, with a balanced field length of less than 1000 feet. In addition to powered lift devices, such an aircraft will need some auxiliary means to elevate the nose during takeoff and landing at very low flight speeds. The RALS concept meets this need and is therefore a strong contender for STOL as well as V/STOL aircraft.

This study covered the modifications to the existing STOL fighter model needed to simulate a RALS-powered V/STOL configuration. Specific modifications include the adaptation of two-dimensional lift/cruise nozzles on the nacelle-mounted J97 engines. This nozzle design, developed under NASA Contract NAS2-10127, features a single-ramp flowpath for cruise and STOL operation, and an internally vectored flowpath for vertical operation.

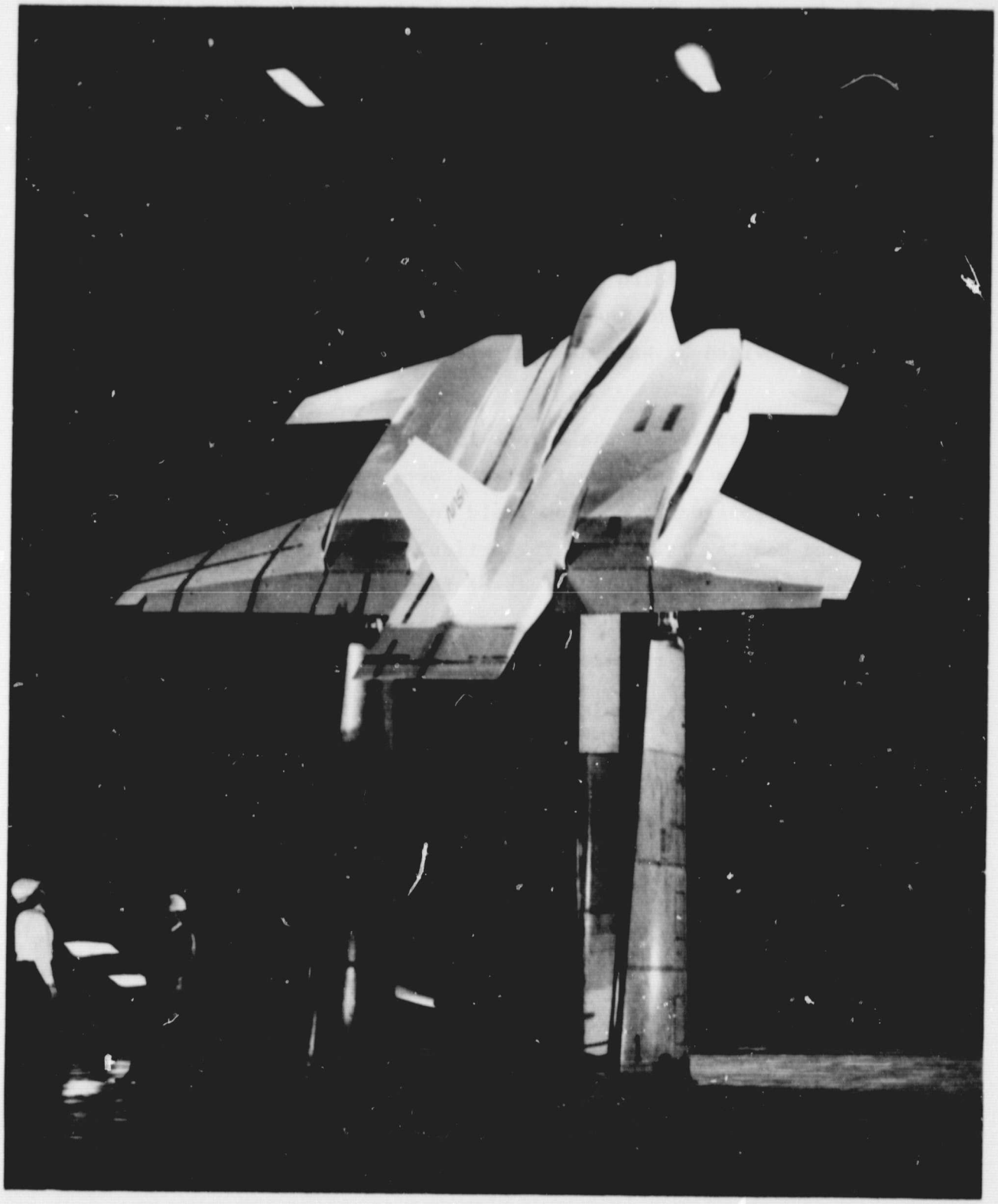

Figure 1. Large-Scale STOL Fighter Model.

The simulation of a RALS nozzle required the addition of a third J97 engine mounted backwards in the fuselage. The nacelle inlets are enlarged to supply air through a plenum to the third engine. The exhaust from this engine is ducted forward in the aircraft and discharged through a vertical nozzle that may be located in either the two axial locations, typical of different aircraft designs. This approach is intended to provide sufficient flexibility to explore ground effects and reingestion in the vertical operating mode.

The addition of the third engine will require extensive structural modification and recontouring of the fuselage and wing root areas. This design effort will be provided by NASA-ARC and was not included in the contracted study.

It was desired to locate the inlets for the third engine adjacent to the present nacelle inlets to provide realistic aerodynamic moments on the model and to achieve a representative flow field for reingestion. This resulted in rather long and complex inlet ducts. Particular attention was given to this area of the redesign. A detailed study of the J97 engine distortion sensitivity was conducted providing guidance for the selection of an inlet screen, operating procedures, and recommendations of inlet instrumentation.

A detailed design was completed of the exhaust ducting and remote nozzle. Materials and fabrication techniques were selected for these components that are consistent with NASA-ARC shop capability. Detailed hardware drawings have been provided for the fabrication of these parts.

3.0 CONCEPTUAL DESIGN

The conceptual redesign of the STOL fighter model included the integration of lift/cruise nozzles into the nacelles and the addition of the third engine and associated ducting to the fuselage. Extensive modifications are required to the fuselage, wing roots, and nacelle components of the model to accommodate these added functions.

3.1 DESIGN REQUIREMENTS

To establish requirements for the RALS simulation, a number of aircraft companies that had conducted design studies of V/STOL fighters were contacted. Six preliminary aircraft designs have been made by the following design teams:

General Dynamics - Fort Worth Division

Grumman Aerospace Corporation

Northrop

McDonnell Aircraft Company

Vought Corporation

Naval Air Development Center - Warminster, Pa.
(Aerodynamics and Propulsion Division)

Their needs varied considerably as indicated in Table I. Generally, those designs in which the remote exhaust nozzle is located behind the pilot needed a thrust split (remote/main nozzle) of about 45/55. These designs in which the nozzle is located ahead of the pilot needed about 35/65 because of the longer moment arm. It was concluded that the GE16/VVCE5 Study D5 cycle was a good objective for the purpose of setting RALS design requirements. This cycle is briefly described in Table II.

The use of J97 turbojet engines in the model required deviation from these cycles and geometric objectives.

Several design parameters are critical and required careful selection. These parameters include vector angles, jet area to wing area ratio (A_8/A_{wing}),

Table I. Results of Industry Survey.

Aircraft Company	Vector Angle (X-Y), degrees	Vector Angle (Side), degrees	Bay Temp., ° F (° K)	Thrust Mod., %	Thrust Ratio Front-Rear
A	15 Fwd. 30 Aft	±15	420 (489)	Not Specified	35/65
B	20 Fwd. 45 Aft	±15 to 35	Cooling Air Required	±7 Pitch	35/65
C	15 Fwd. 60 Aft	±10	?	±25 Landing ±20 TO	39 - 61 41 - 59
D	15 Fwd. 35 Aft	±6	800 (700) For T1 550 (561) for Composites	±10	45-55/55-45
E	20 Fwd. 30 Aft	±15	T_{BAY} Low Enough for Insulated Composites	±9.2	40/60
NADC	0 Fwd. 90 Aft	±10	Not Specified	±10	32/68

Table II. SYS GE16/VVCE5 Study D5.

W_a	200 lb/sec (90.7 kg/sec)
F_N (Max. Vert.)	17,866 lb (79,468 N)
F_N Split	45/55
P/P Fan	4.0
OPR	28
Bypass Ratio	1.0
T_{41} Max.	3200° F (2033° K)
T_{EXH} Max.	2800° F (1811° K)
Bleed	9 lb/sec (9% Core) (4.1 kg/sec)
$WT_{Eng} + WT_{RALS}$	2850 + 200 = 3050 lb (1383 kg)

and jet velocity ratio (V_{jet}/V_o). The latter parameter has been used to nondimensionalize jet-induced effects in most previous studies. It directly influences jet penetration and shape in the free stream, and can be influenced to some extent by differential operation of the engines and tunnel.

The General Dynamics RALS turbofan-powered Model R-104 aircraft design has been examined along with the existing STOL fighter windtunnel model. It was concluded that the existing model is not an exact geometric scale of the V/STOL aircraft design of Contract NAS2-9796 as shown in Table III.

Table III. Comparison of General Dynamics Model R-104 and STOL Model Characteristics.

	R-104	STOL Model	Implied Scale
Wing Area	300 ft^2 (27.9 m^2)	183 ft^2 (17 m^2)	0.78
Aspect Ratio (AR)	3.6	3.1	---
Semispan (b/2)	197 in. (5.0 m)	143 in. (3.63 m)	0.73
Length	556 in. (14.12 m)	403 in. (10.24 m)	0.72
Canard (AR)	2.1	2.4	---
A_{RALS}/A_{wing}	0.0108	---	---
A_{Noz}/A_{wing}	0.0154	0.010	---
V_{RALS}	3160 ft/sec (963 m/sec)	2810 ft/sec (856 m/sec)	---
V_{Noz}	3108 ft/sec (947 m/sec)	---	---

The ratio of exhaust nozzle area (A_{Noz}) to wing area (A_{wing}) is somewhat lower in the STOL model, reflecting the dry turbojet engine geometry. An optimum simulation would require either a much smaller wing or larger jet area. It was decided that a new wing and canard combined with all the fuselage changes needed to obtain full simulation would constitute almost a new model and not be an attractive alternative. A larger jet area could be provided by the addition of an augmentor, but this is also beyond the scope of the program. The exhaust velocity, which is a function of nozzle pressure ratio, is somewhat lower for the dry turbojet, but still within the range of interest. It is also noteworthy that the 50% increase in inlet area needed to supply a third engine would make the inlet geometry more representative of a turbofan engine than it is in the current model.

A planform of the model modified to include the fuselage-mounted J97 engine is shown in Figure 2. Alternate axial locations of the remote nozzle are shown to simulate the two general locations selected by the aircraft designers.

3.2 LIFT CRUISE NOZZLE DESIGN

The lift/cruise nozzle design developed under NASA Contract NAS2-10127 was incorporated into the V/STOL large-scale fighter model. This nozzle design, shown in Figure 3, features a two-dimensional single-ramp flowpath for cruise and STOL as well as an internally vectored flowpath for VTOL. A dual cowl flap provides A_8 and A_9 control and serves as a blocker during VTOL. The nozzle is integrated with the aircraft wing flap which is independently variable to provide partial jet vectoring up to ±30°. This system also features an engine flow diverting system which is capable of supplying up to 16% of the engine flow to a wing spanwise blowing nozzle. This flow diverting system is located upstream of the nozzle as shown in Figure 4.

Sizing of the J97 exhaust system was performed based on the test plans defined by NASA-ARC (Table IV). The effective nozzle area was selected as 117.6 $in.^2$ consistent with previous test operation to 95% speed and a nozzle pressure ratio of 2.7. The top speed of 95% was selected in order to increase the engine life.

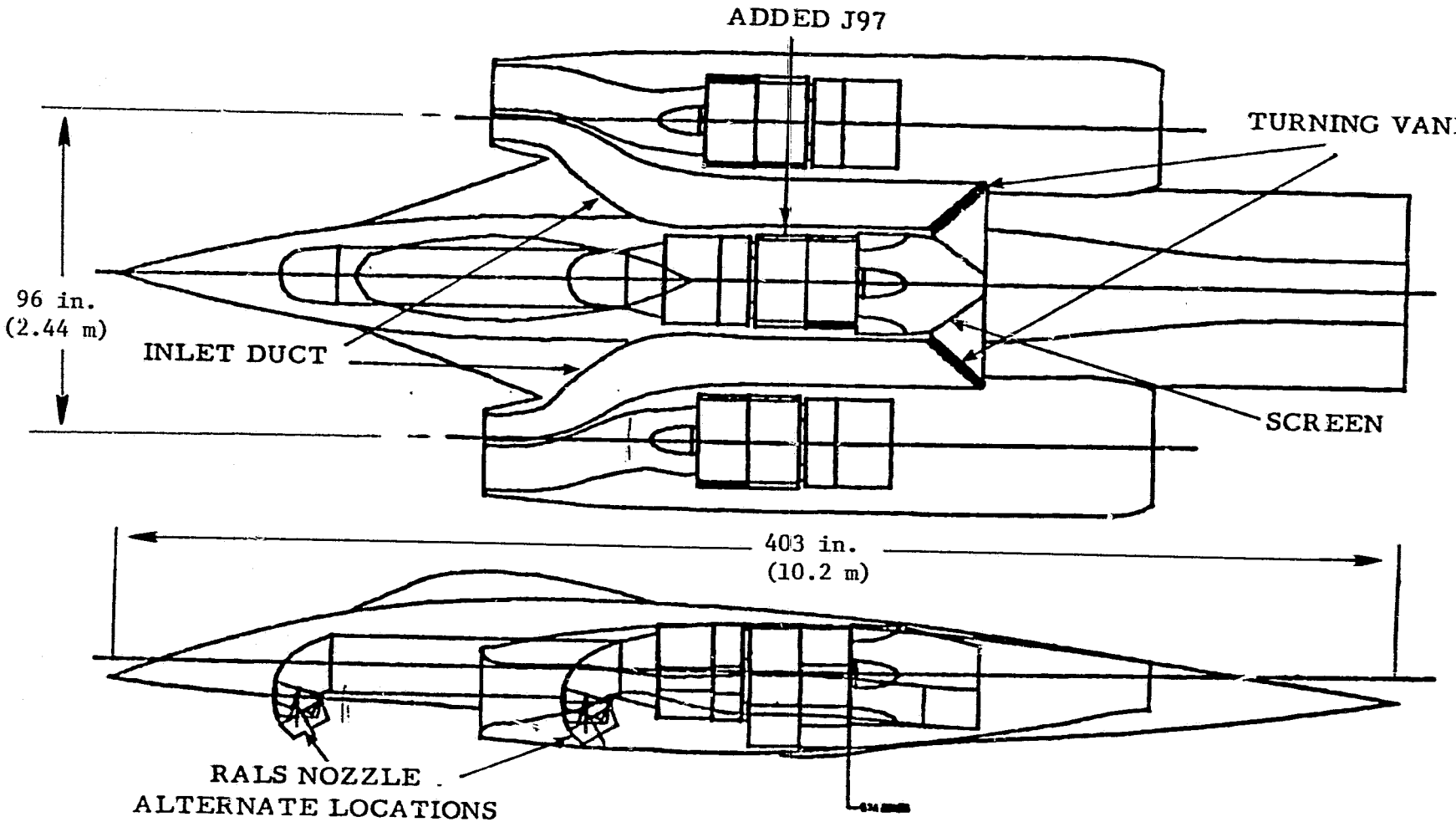

Figure 2. Proposed STOL Model Modifications.

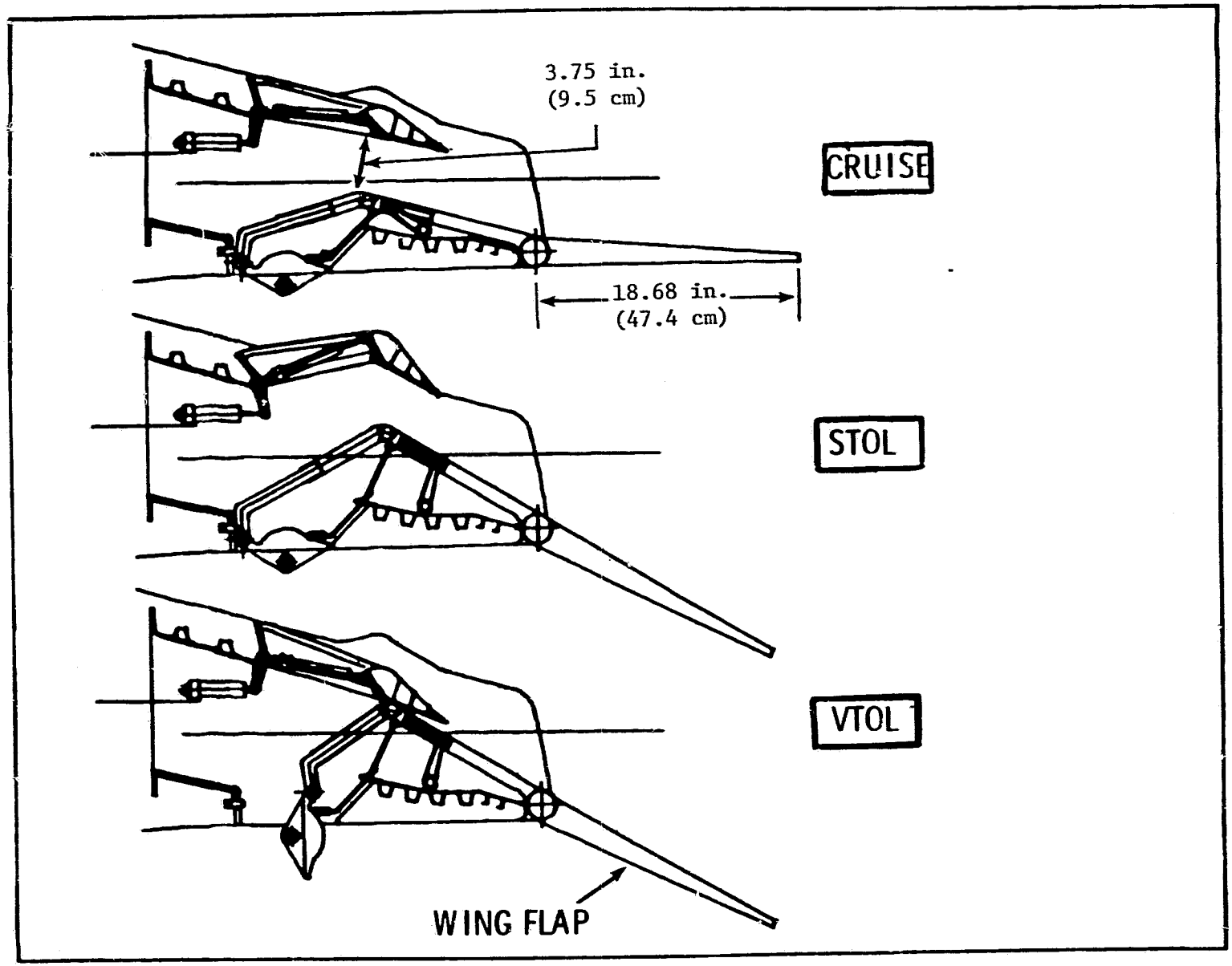

Figure 3. NASA V/STOL Model Lift/Cruise Nozzle.

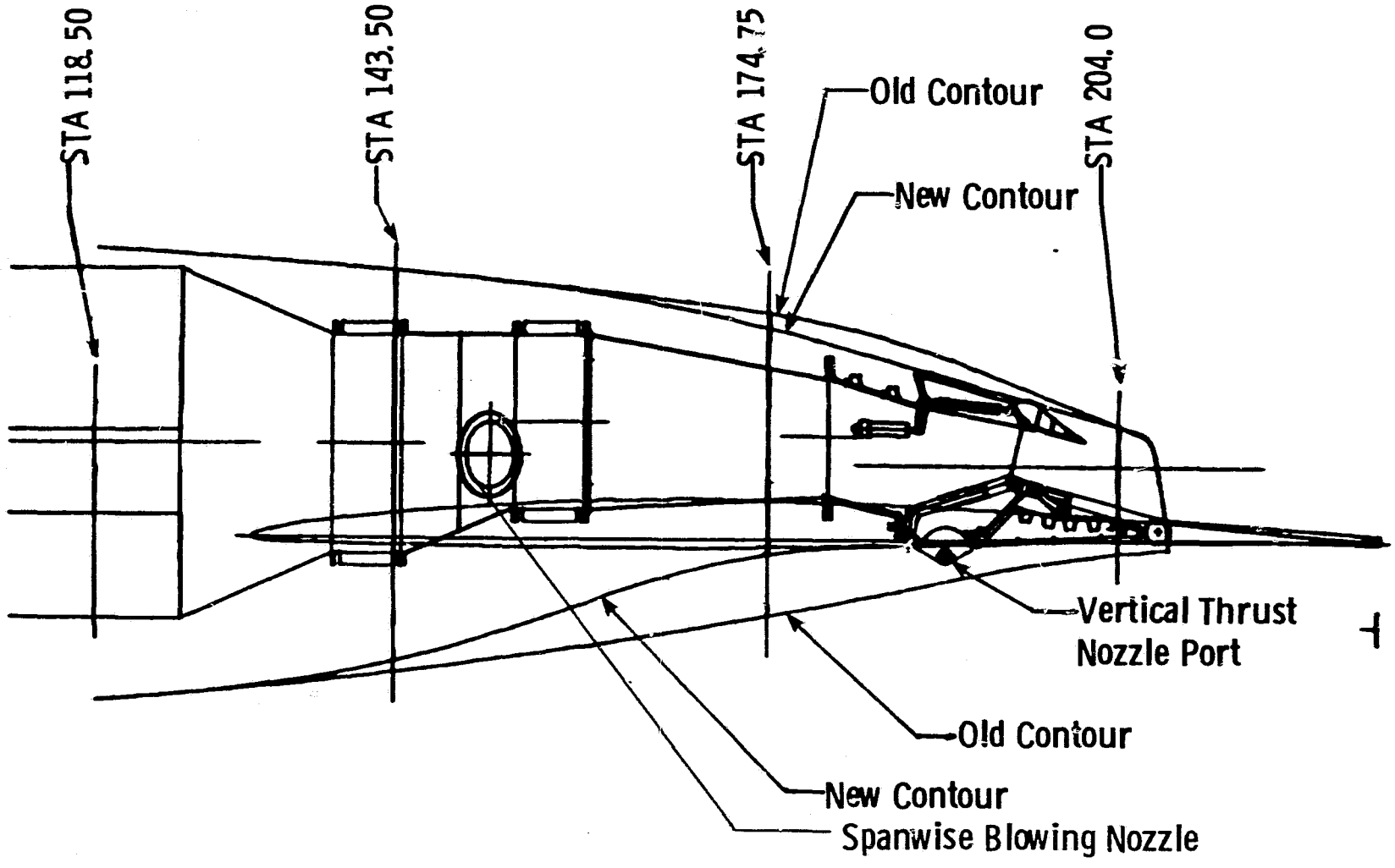

Figure 4. V/STOL Exhaust Nozzle.

Table IV. NASA-ARC Test Plans-RALS V/STOL Model.

	VTOL	STOL	Cruise
P_8/P_o	1.6-2.6	1.6-2.6	2.0-2.6
Tunnel Velocity, knots	0-20	40-120	100-180
Angle of Attack, α, degrees	-4/+6	-4/+40	-4/+12
Yaw Angle, degrees	0/+25	-15/+30*	-10/+10

*to α = 12

The physical and effective areas selected for the cruise, STOL, and VTOL positions are tabulated in Table V. An effective area of 117.6 in.^{2} was also selected for the cruise and VTOL positions. The estimated discharge coefficient for the cruise mode is approximately 0.98 based on existing test data; and, therefore, the physical throat area was defined as 120 in.^{2}. The nozzle width is 32 in. for the model, so the throat height was set at 3.75 in. The flow coefficient in the VTOL configuration cannot be readily determined due to a lack of test data. Therefore, General Electric recommends that NASA-ARC allow provision in the design to cut back or lengthen the forward lip piece to obtain the required effective nozzle area. The VTOL configuration is initially sized for a 0.75 flow coefficient in Table V. For STOL operation, the spanwise blowing system would be used with a geometric area of 20 in.^{2}. Assuming a 0.95 discharge coefficient for the spanwise blowing system, the effective primary throat area was set at 98.6 in.^{2}, which translates into a physical throat area of 100.6 in.^{2} based on a 0.98 discharge coefficient. Considering a 32-in. width, the throat height is 3.144 in.

Table V. Exhaust Nozzle Area Requirements.

Nozzle Position	A_{8} in.^{2}	A_{e_8} in.^{2}	A_{SWB} in.^{2}	$A_{e_{SWB}}$ in.^{2}	$A_{e_{Total}}$ in.^{2}
Cruise	120.0	117.5	0	0	117.6
STOL	100.6	98.6	20	19	117.6
VTOL	156.8	117.6	0	0	117.6

In Figure 4, the old and new nacelle contours are compared. The revised contour was necessary because of STOL model restrictions. The main difference is on the lower contour where it was necessary to increase the boattail angle significantly in order to properly install the nozzle in the VTOL position.

Performance predictions for these lift/cruise nozzles were made based on the performance estimates developed under NASA Contract NAS2-10127. The only difference affecting performance between this nozzle design and that developed under the previous NASA contract is the length of the wing flap. The chord of the wing flap is about twice as long as desired from a nozzle point of view; and as a result, the thrust coefficient was reduced by 1.5%. This is based on static test data which shows that the performance is reduced 1% to 2% as a result of lengthening the upper ramp. The performance predictions for the cruise, STOL, and VTOL positions are as follows:

Nozzle Position	Thrust Coefficient
Cruise	0.955
STOL	0.955
VTOL	0.945

Note that these performance estimates include the effect of leakage as calculated for NASA Contract NAS2-10127. These predictions are for a nozzle pressure ratio of 2.6.

3.3 INLET DESIGN

The inlet flowpath design for the third YJ97, as well as the resultant redesign of the inlets for the two outboard engines, was strongly influenced by several NASA requirements:

- STOL model planform changes were to be minimal.
- Third engine/outboard engine inlet openings were to be common.
- Inlet faces were to be normal to engine centerlines (normal shock inlets rather than the oblique shock inlets used in previous STOL model).

Other NASA requirements included retaining the existing strake geometries, as well as leaving fuselage structure upstream and downstream of the third engine unchanged. The cooling air scoops used in the previous inlets for nacelle cooling were eliminated, simplifying the addition of the third engine inlet openings.

Starting with these requirements, an axial location was selected for the third engine consistent with RALS system and NASA structure considerations. The flowpath from the leading edge of the previous inlets to the third engine was then defined. Sizing and shaping of the inlet flowpath from the inlet face into and through the model strakes were performed with the aid of the Interactive Graphic System (IAGS). This design process resulted in a flowpath with a constant Mach number of 0.32. To facilitate flow turning from the strake duct through 180° into the plenum, the following design features were incorporated. Local Mach numbers were reduced where possible - from 0.32 in the strake duct to 0.28 going into the first 90° turn, to 0.23 going into the second turn, and to 0.13 in the plenum. Seventeen turning vanes were used in the first turn. A FOD/turbulence damping screen (scaled from a previously employed General Electric design) was added in the second turn comprising the forward extension of the plenum. The purpose of this high density screen is twofold: first, it will provide damping and redistribution of flow differences

created in the two inlet ducts by simulated maneuvers (angle of attack, yaw); and second, it will smooth out flow distortion created by the forced geometric arrangement. This arrangement dumps flow into the plenum from two "small" rectangular ducts located off-center into a "large" axisymmetric plenum (Figure 2). Although the high density screen (35% porosity) is expected to exert substantial influence on reducing flow distortion, additional distortion reduction is expected from flow acceleration (0.13 plenum Mach number to 0.35 compressor face Mach number) and from the presence of the seven front frame struts in the YJ97.

Total pressure losses for this inlet system were estimated to be 10.5% (at 55 lb/sec corrected engine flow). Approximately 35% of this loss is attributable to the FOD screen.

Other considerations in the design of the inlet system were the avoidance of flow separation at high angles of attack and yaw and the avoidance of excessive hot gas reingestion in the vertical operating mode. These concerns were addressed as follows. Generous lip radii are employed for the inlets to provide tolerance-to-flow angularity. No mechanical or aerodynamic problems are expected with this approach.

Hot gas ingestion can be expected to be a problem with the inlets located near the remote nozzle discharge. In a VTO aircraft design, this problem would probably require the use of auxiliary inlet doors in a protected area such as on top of the nacelles. This configuration can be readily simulated in the V/STOL model by substituting top-entry inlets as shown in Figure 5 during VTO operation. Preliminary estimates of total pressure loss in the top-entry inlets is 2% greater than in the conventional inlets at 55 lb/sec corrected engine airflow.

Because of the complex geometry of the inlet system, either scale model testing or full scale testing of the system is recommended prior to engine operation. On the basis of this testing, the porosity of the inlet screen can be adjusted to achieve a proper balance between induction pressure loss and distortion at the engine face.

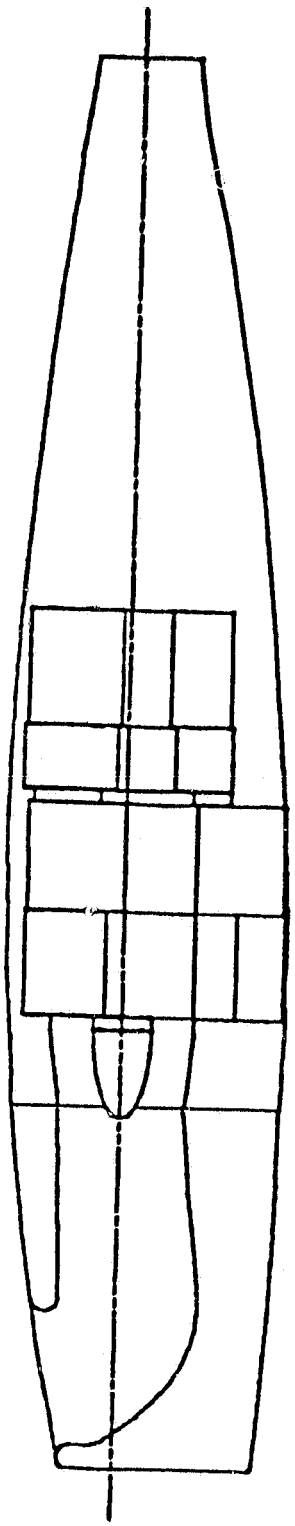

Figure 5. Top-Entry Inlet Duct Geometry.

3.4 INLET DISTORTION ANALYSIS

The stability limit of the J97 engine with respect to inlet pressure and temperature distortion was evaluated analytically to permit making an estimate of the system operational capability. In order to determine the pressure and temperature distortion limits, the installed operating surge margin and associated internal destabilizing influences were established. A map of the compressor is shown in Figure 6 with the estimated, nondistorted surge line indicated. Estimated operating characteristics of the installation were obtained from a computer model (cycle deck). Since the exact total pressure losses of the inlet system were not known, cycle data were generated for 95%, 85%, and 75% recovery with the exhaust nozzle (A_8) sized at 110.6 in.^{2} and a flow coefficient of 1.0.

The speed/airflow characteristic for the three inlet recovery conditions is shown in Figure 7. The operating pressure ratio/airflow characteristic relative to the nominal surge line is shown in Figure 8 and the calculated available surge margin is shown in Figure 9. The minimum available surge margin condition (75% inlet recovery) representing the highest estimated inlet total pressure loss was used for further evaluation to determine the pressure and temperature distortion limits. This represents the most pessimistic viewpoint since the actual inlet recovery is expected to be better than 75%.

Starting with the nondistorted surge margin from the cycle deck as the nominal available, an accounting of internal destabilizing effects was made to determine the net remaining margin for external effects (distortion). The internal effects (deterioration, control tracking and thermal) accounted for in this installation represent the expected changes for the test period. The accounting procedure shown below provides for predictive (direct summation) and random (room sum squared) effects as well as for the difference in operating condition. The following definitions were used:

Surge Margin Available (SM_A) @ Flow = Constant

$$SM_A \equiv \left[(P/P)_{Surge} - (P/P)_{Op.\ Line}\right] / (P/P)_{Op.\ Line}$$

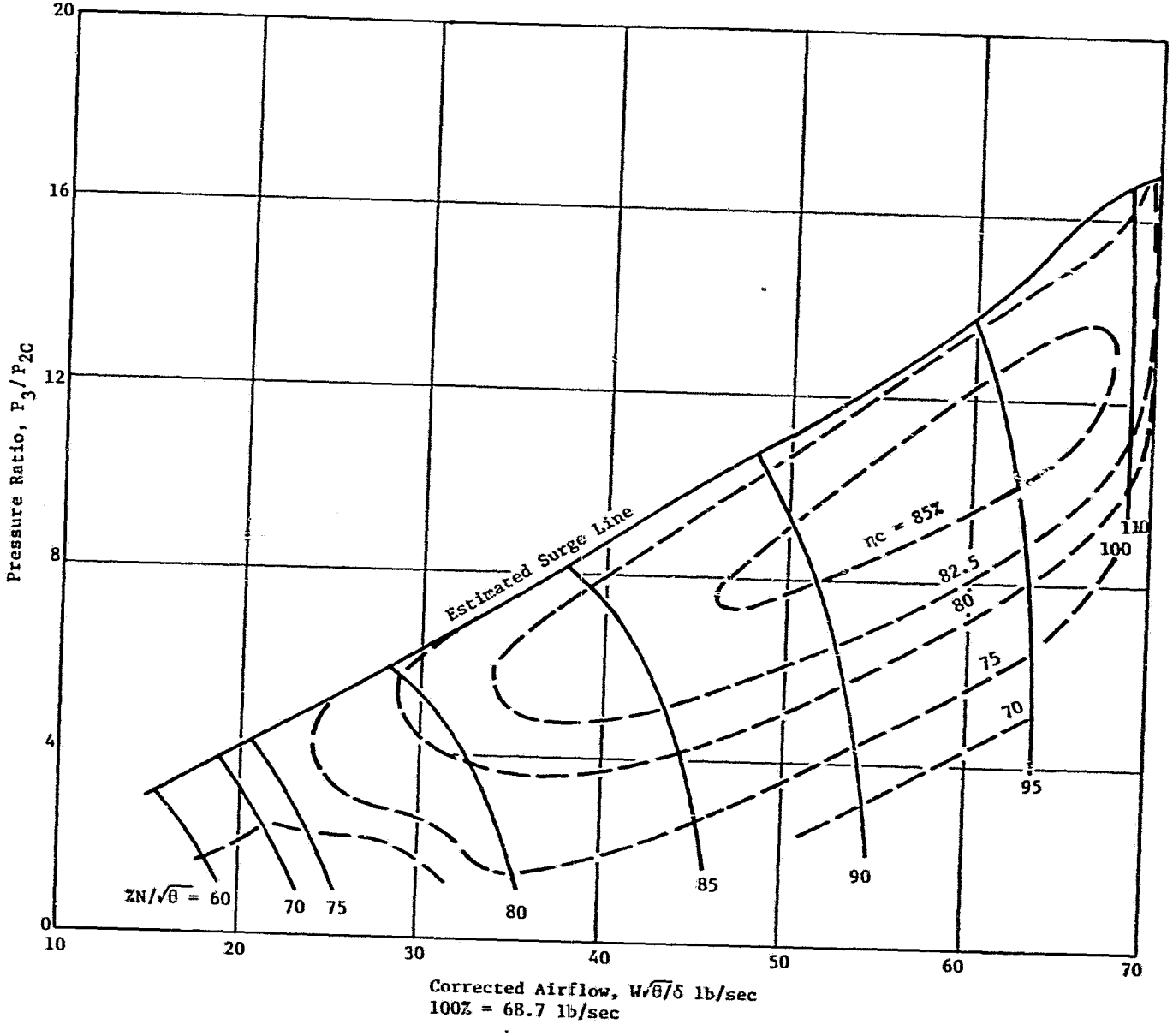

Figure 6. J97-100 Compressor Map.

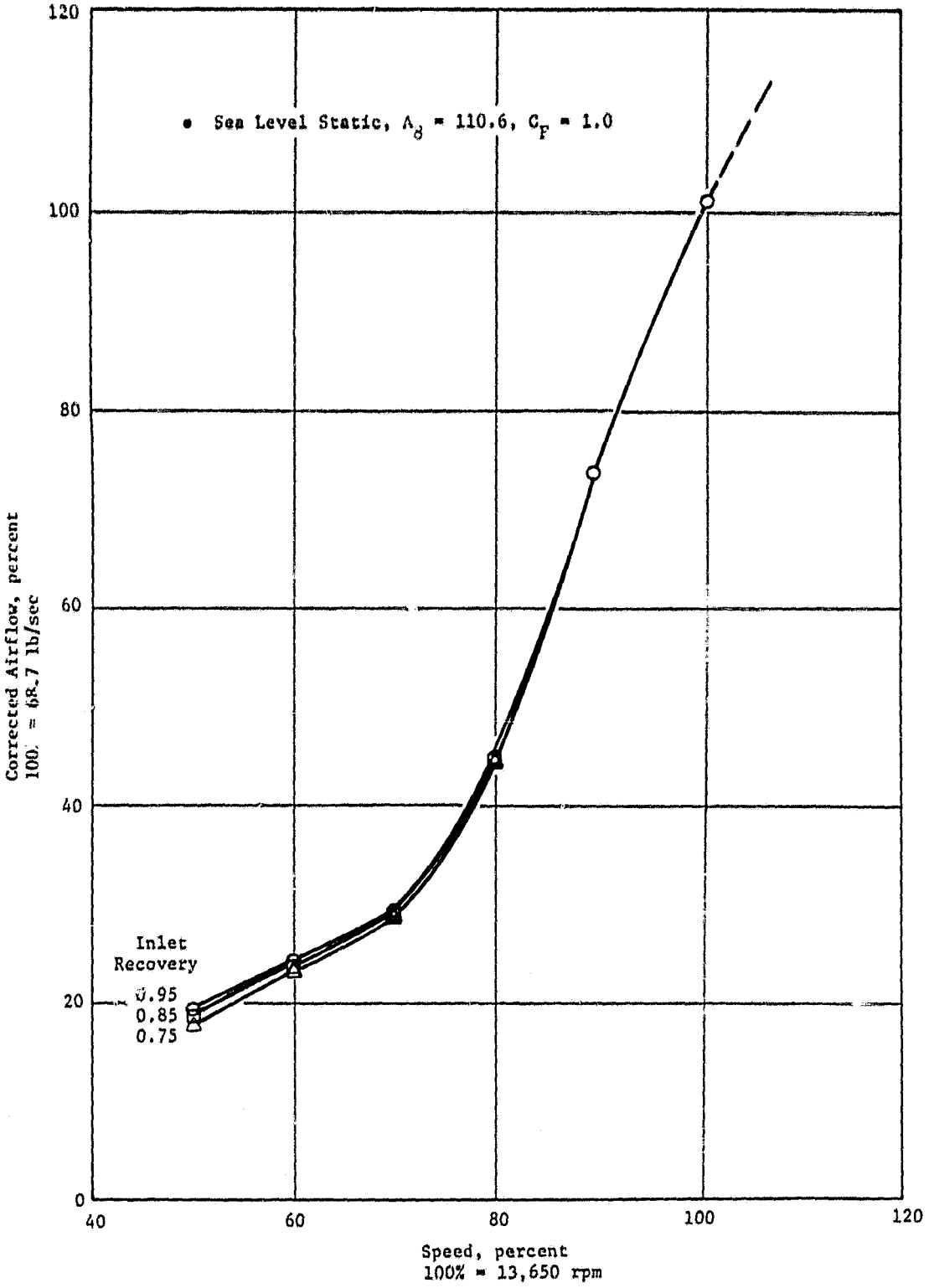

Figure 7. J97-100 Compressor Speed/Flow Characteristics.

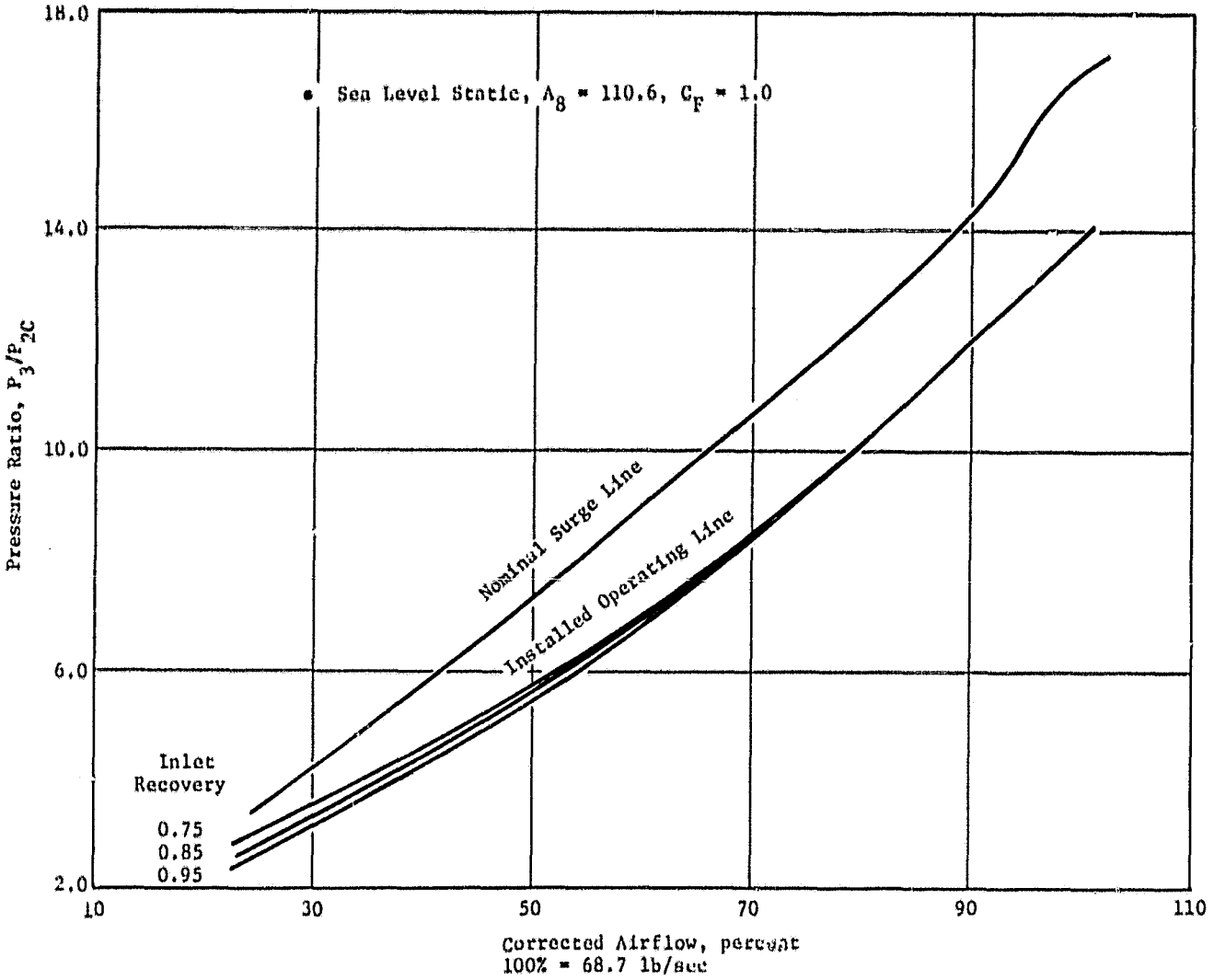

Figure 8. J97-100 Compressor Operating Characteristics.

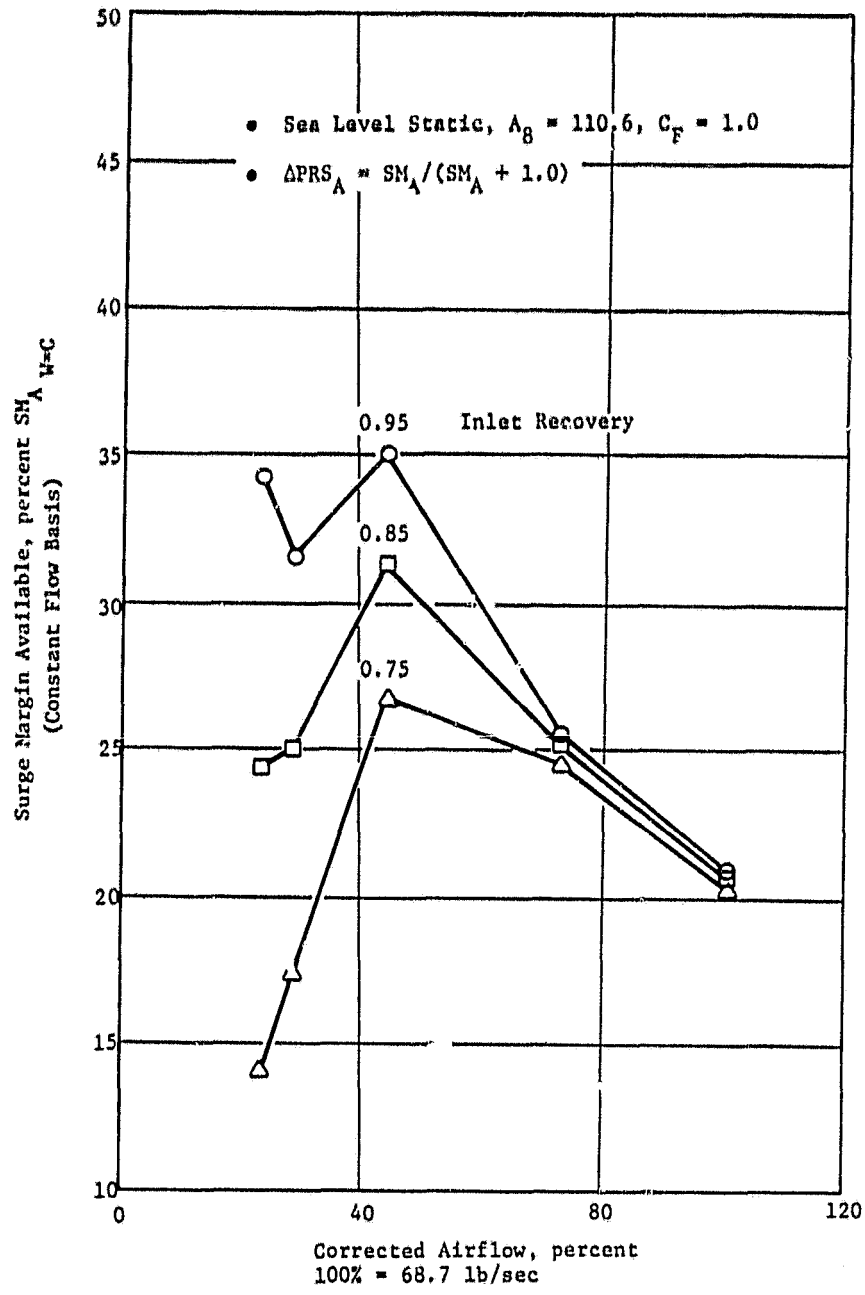

Figure 9. J97-100 Surge Margin Available.

Surge Pressure Ratio Loss Available (ΔPRS_A)

$\Delta PRS_A \equiv SM_A / (SM_A + 1.0)$

Internal Surge Pressure Ratio Loss (ΔPRS_I)

$\Delta PRS_I \equiv$ Stackup from Table VI.

Table VI. Compressor ΔPRS_I Stackup.

% Corrected Airflow	30		80		100		105	
ΔPRS Loss Item	Δ	RSS	Δ	RSS	Δ	RSS	Δ	RSS
Op. Line Var.		0.003		0.007		0.008		0.008
Surge Line Var.		0.005		0.016		0.020		0.020
Stator Track	0.010	0.010	0.010	0.010	0.010	0.010	0.010	0.010
Deterioration	0.010		0.010		0.010		0.010	
Thermal Effect	0.005		0.005		0.025		0.025	
	0.025+0.012		0.025+0.020		0.045+0.024		0.045+0.024	
Steady State ΔPRS_I	0.037		0.045		0.069		0.069	
Power Transient	0.067		0.049		0.021		0.021	
Fuel Schedule Var.		0.012		0.012		0.012		0.012
	0.092+0.017		0.074+0.023		0.066+0.027		0.066+0.027	
Throttle Movement ΔPRS_I	0.109		0.097		0.093		0.093	

Two different levels of internal margin usage were determined (steady state and throttle movement) since actual test procedures were not defined. If snap throttle changes (Δ throttle $\leq$ 0.5 sec) are not planned, the distortion capability of the engine is increased, since the net margin for distortion (ΔPRS_D) is the difference in nominal available and that allowed for internal effects. $\Delta PRS_D \equiv \Delta PRS_A - \Delta PRS_I$ (Figure 10) shows the total allowance for internal loss effects for both steady-state and throttle movement.

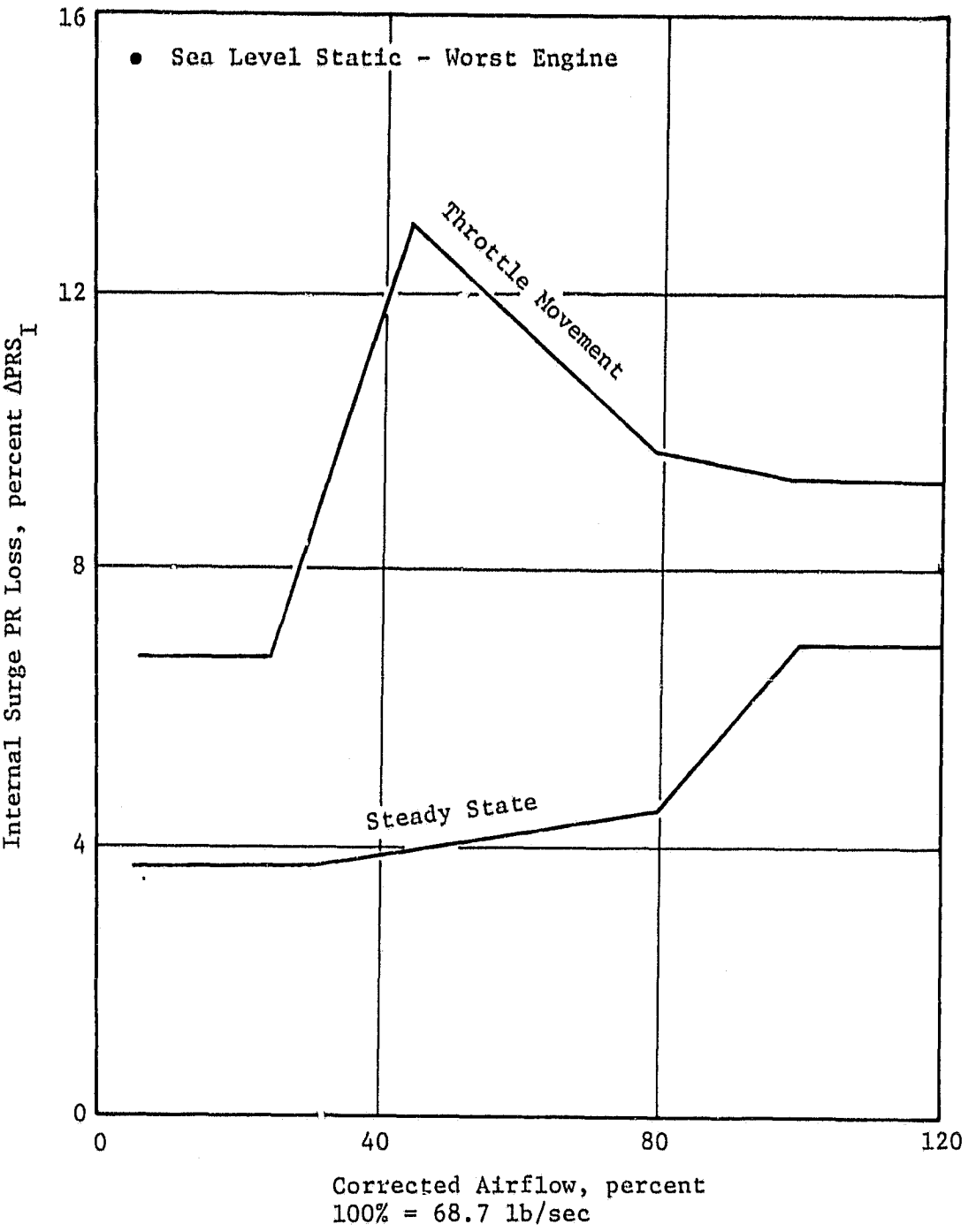

Figure 10. J97-100 Compressor Stack.

With the net margin for distortion (ΔPRS_D) defined, the sensitivity of the engine to both types of expected distortion (pressure and temperature) was evaluated. Results from past tests, comparable component information, and theoretical analysis provided the data to establish the individual sensitivity characteristic. Since most of the past information was in terms of obsolete parameters, a simple definition of distortion was used instead of converting to current indices. The parameters for pressure distortion and temperature distortion were:

$$(\Delta P/P)_{Max} = (P_{Max} - P_{Min})/P_{Avg}$$

$$(\Delta T/T)_{Max} = (T_{Max} - T_{Min})/T_{Avg}$$

These parameters also provide convenience/ease of measurement/monitoring for excess levels during test. Instrumentation recommendations and typical design drawings have been provided. Figures 11 and 12 show the resultant sensitivity of the compressor (loss in surge pressure ratio per unit of distortion) for pressure distortion (K_p) and temperature distortion (K_T), respectively.

A simple linear equation for estimating the loss in margin $\Delta PRS_D = K_p(\Delta P/P)_{Max} + K_T(\Delta T/T)_{Max}$ provides the means, by mathematical manipulation, to determine the limit distortion for this installation. For steady-state operation, Figure 13 shows the various combinations of pressure and temperature distortion estimated as the limit capability as a function of engine operating condition. For zero temperature distortion, the pressure distortion limit is 30% $(P_{Max} - P_{Min})/P_{Avg}$ above 80% corrected airflow but reduces for lower power conditions. As the temperature distortion increases, the pressure distortion limit decreases as shown. Figure 14 shows the same limit characteristic except at lower levels since it includes the allowance for snap throttle movement.

This inlet distortion analysis has resulted in limit definitions and operability restrictions (throttle movement rate) to ensure that there is no engine stall that would interfere with intended model testing. Instrumentation should be installed (minimum recommendation shown in Figure 15) to monitor both pressure and temperature distortion, thereby protecting against excess levels.

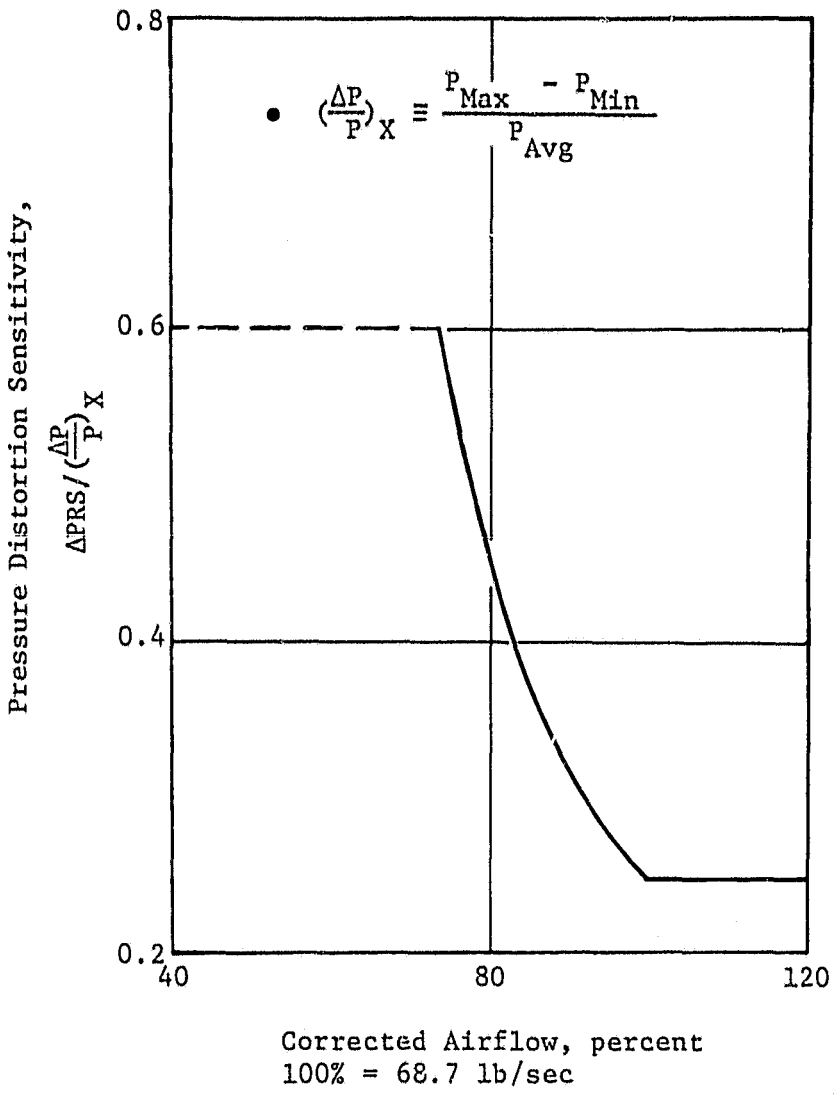

Figure 11. J97-100 Compressor Estimated Pressure Distortion Sensitivity.

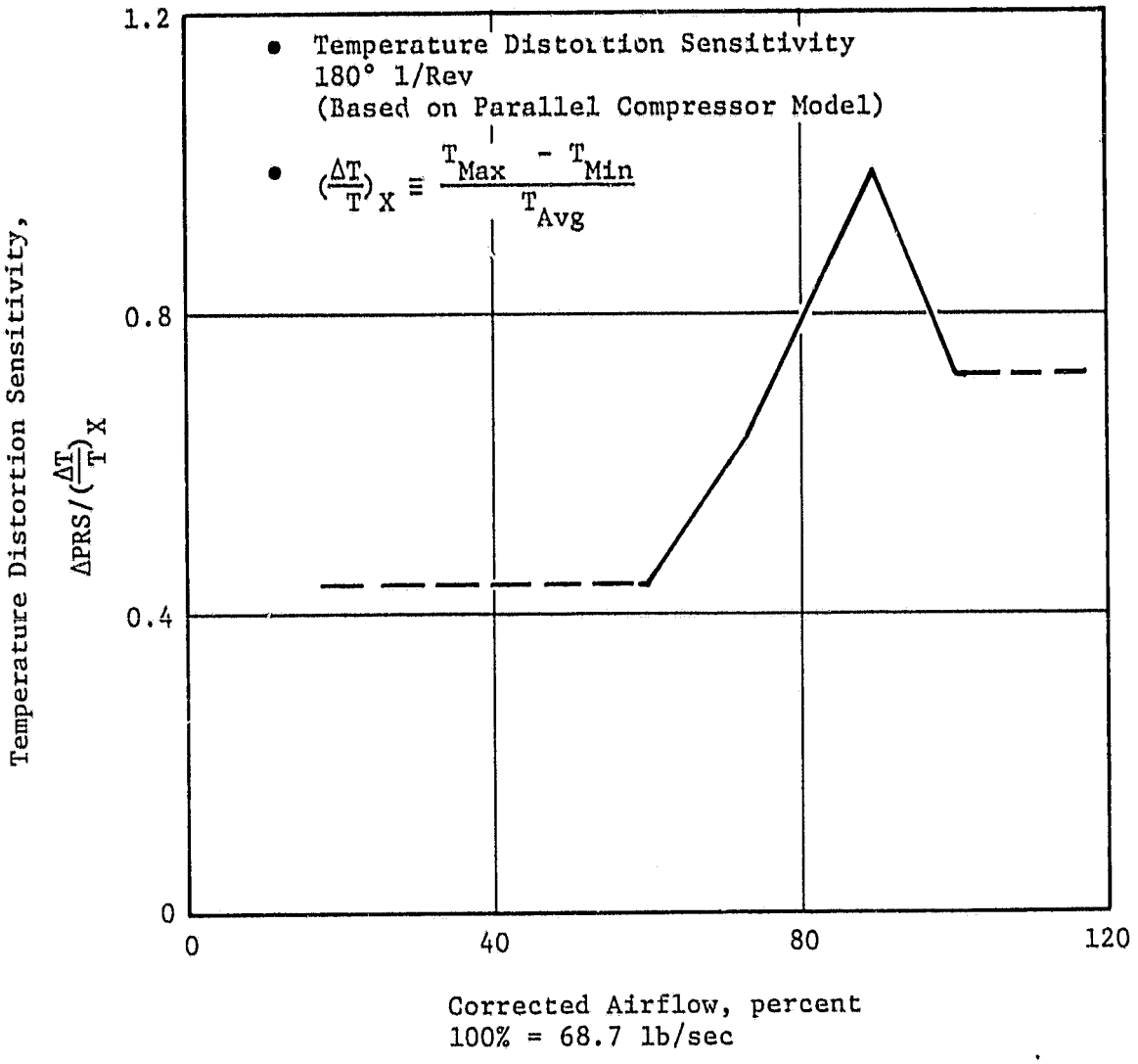

Figure 12. J97-100 Compressor Estimated Temperature Distortion Sensitivity.

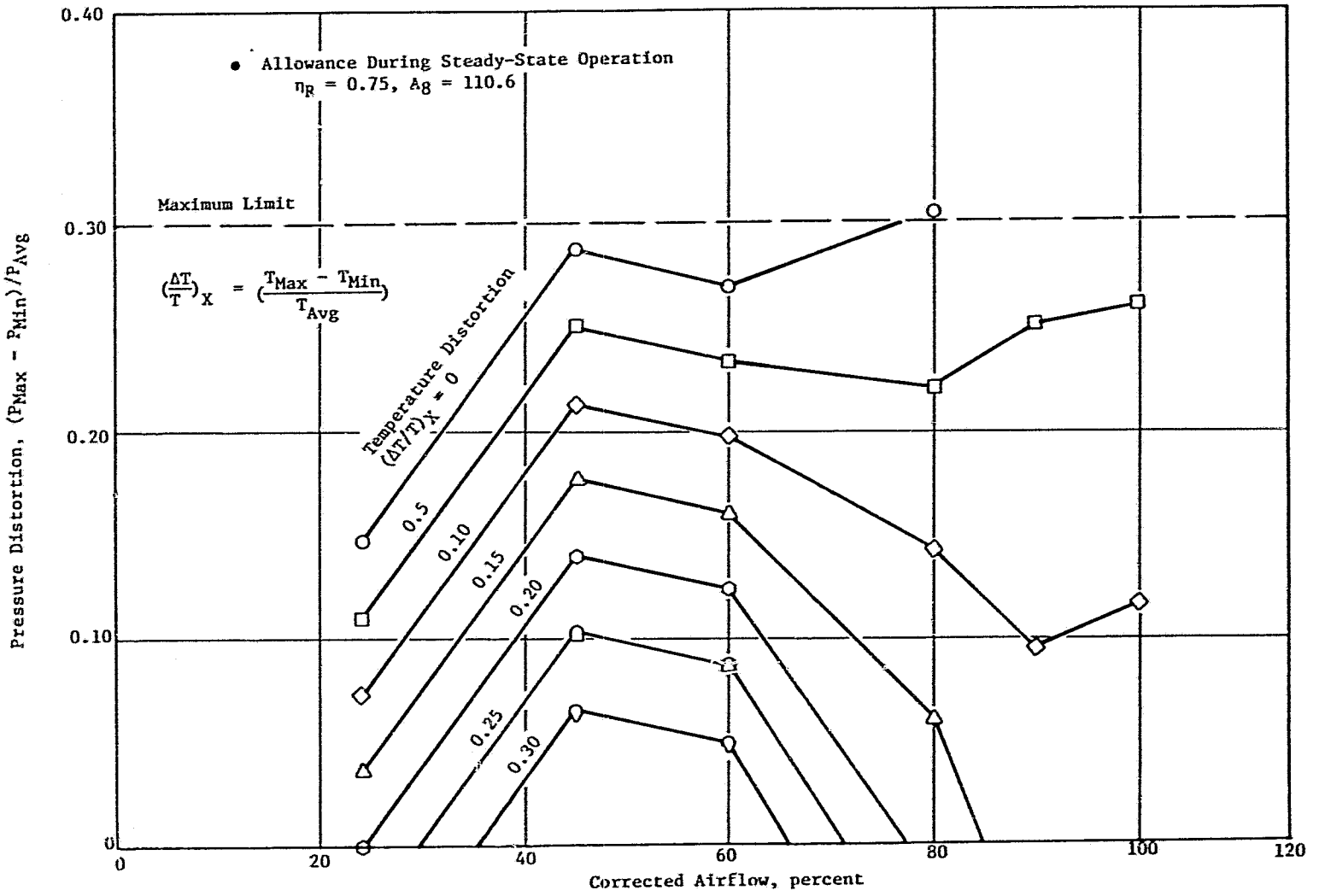

Figure 13. J97-100 Estimated Distortion Allowance During Steady-State Operation.

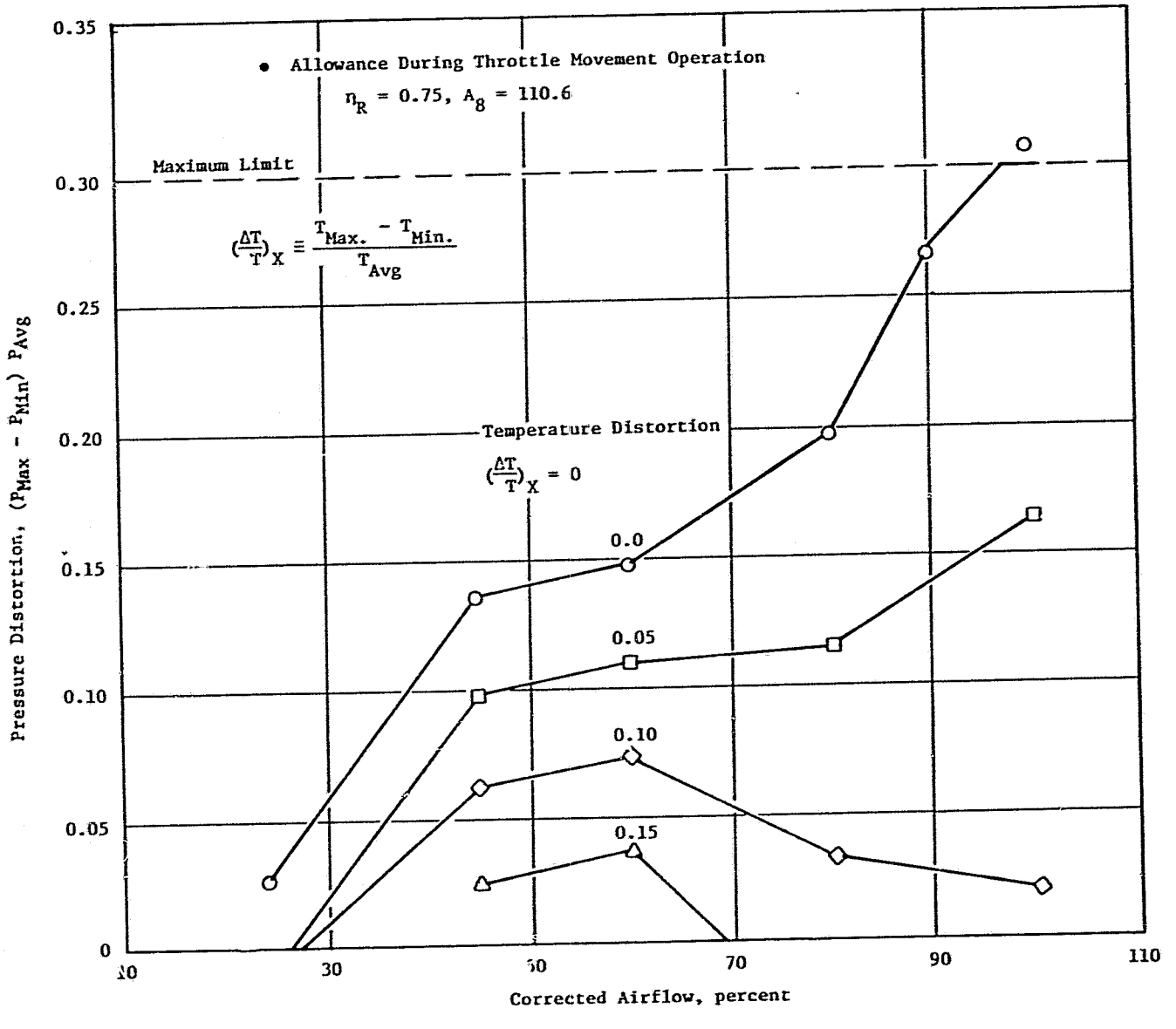

Figure 14. J97-100 Estimated Distortion Allowance During Throttle Movement Operation.

Distortion Methodology

- SAE ARP 1620 Recommends 8 X 5 Measurement to Map Inlet Characteristics
- Requirement for this Test - Monitor for Excess Levels and Prevent Engine Instability

Recommendation

- ○ Steady-State Pressure
  4 X 5 Measurements Provide Eight Locations
- ⬡ Steady-State Temperature
  4 Measurements
  $\tau \approx 0.010$ sec
- △ Dynamic Pressure
  4 Measurements
  $f_c \approx 250$ Hz

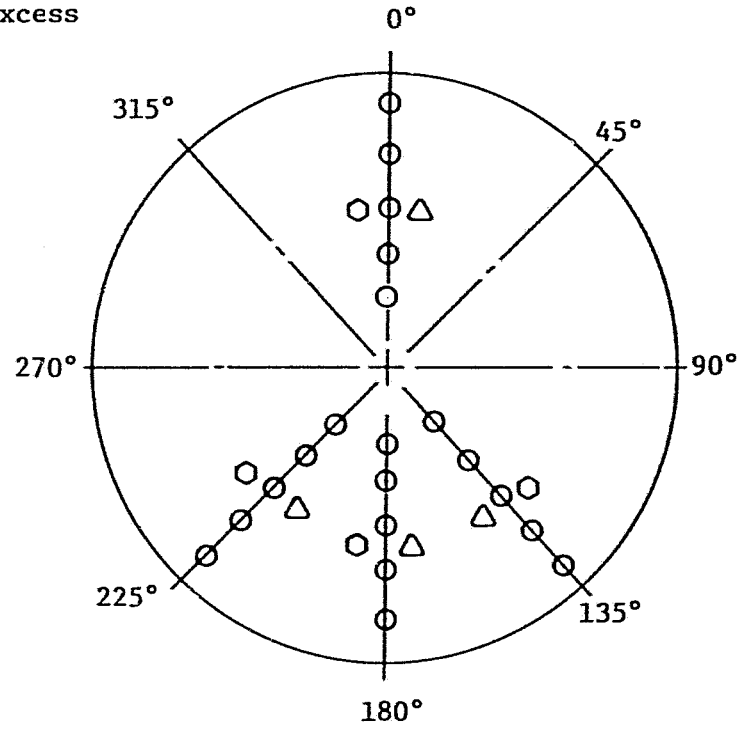

Figure 15. Instrumentation.

3.5 REMOTE NOZZLE LAYOUT

Ducting from the internal fuselage-mounted J97 exhaust to the RALS nozzle is shown in Figure 2. The ducting is designed with provision to attach the RALS convergent nozzle at either of two axial locations. This will allow the V/STOL model to be used to evaluate aerodynamic effects of nozzle axial locations typical of those used in different aircraft design concepts.

A sketch of the ducting flowpath from the J97 exhaust to the aft located RALS nozzle is shown in Figure 16. From the J97 exhaust, the ducting first transitions the flow to a higher duct centerline which is necessary to clear the fuselage lower mold line. The duct Mach number at the end of the transition is 0.42. This Mach number is typical of the duct Mach number used for RALS aircraft designs. The design of the elbow required to turn the ducted J97 flow was based on a US/FRG V/STOL tailpipe design (Reference 5) which has been tested.

The sizing parameter for the elbow is the ratio R_{INT}/R_{DUCT} where R_{INT} is the internal duct turning radius and R_{DUCT} is the duct radius. Both parameters are defined in Figure 16. The US/FRG V/STOL tailpipe design successfully used an $R_{INT}/R_{DUCT} = 0.18$ for the elbow. This ratio was raised to 0.23 for the J97 elbow to account for additional structure in the elbow region.

For the forward RALS location, a cylindrical duct is inserted between the transition section and the elbow. The duct is sized for a 0.42 Mach number.

The RALS convergent nozzle was sized to operate up to a nozzle pressure ratio of 2.7 at a 95% corrected speed, the same as the lift cruise nozzles. Assuming a discharge coefficient of 0.98, the physical throat area was set at 120 $in.^2$, also identical to the throat area of the lift/cruise nozzles. This nozzle was designed to vector the flow at several angles as shown in Figure 2. The nozzle is stowed in the fuselage in the 15° forward vectoring position. For all other vector angles, the convergent nozzle extends below the fuselage.

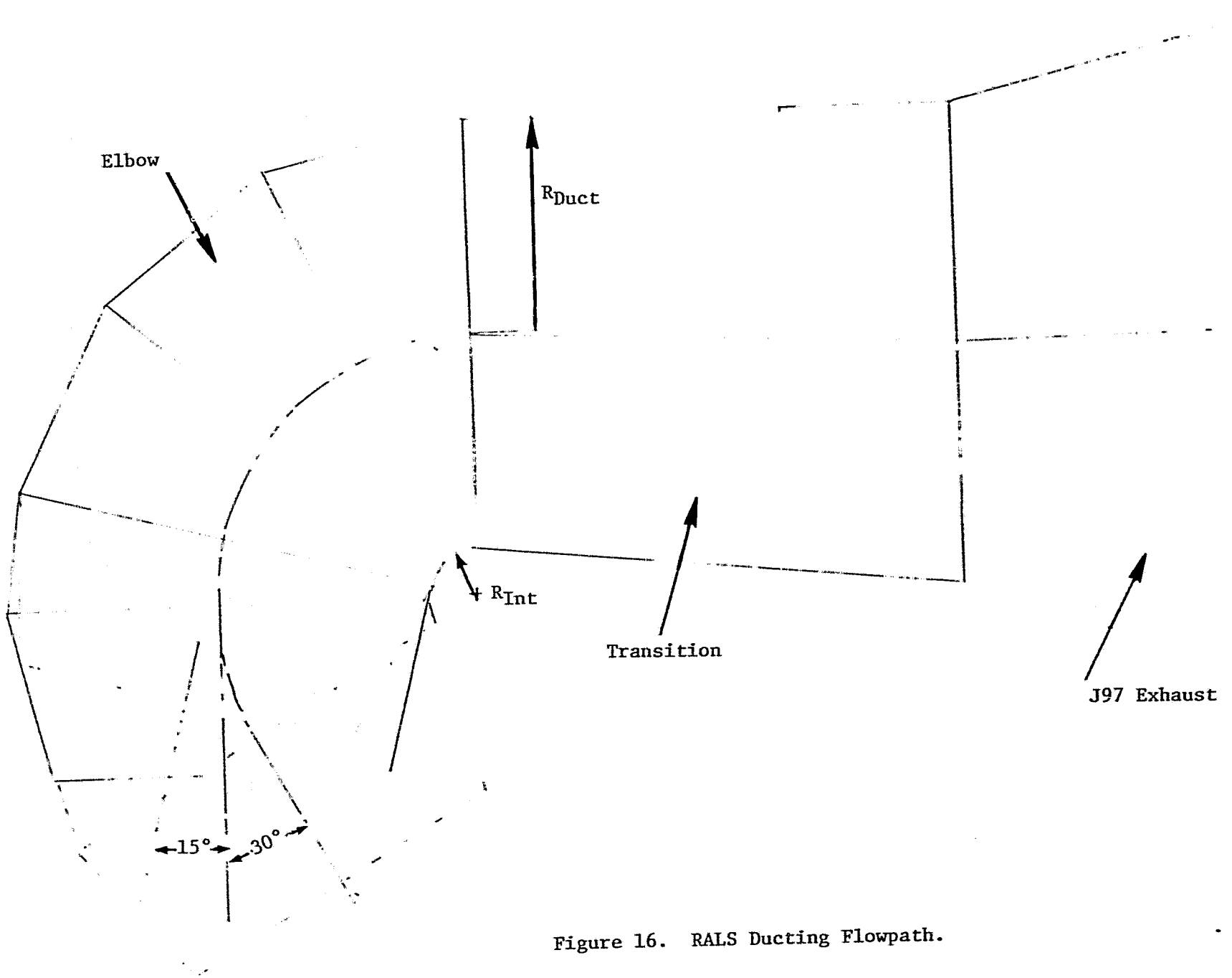

Figure 16. RALS Ducting Flowpath.

4.0 DETAIL DESIGN OF REMOTE EXHAUST SYSTEM

The simulated RALS ducting and exhaust nozzles are shown assembled in Figure 17. The ducting consists of a modified YJ97 engine exhaust diffuser duct, short and long spool sections, a 75° flow turning section, and four interchangeable fixed area nozzles. Installation of the remote nozzle assemblies in the NASA-ARC large-scale fighter model is depicted in Figure 18.

The two spool sections are used to change the axial vectored thrust station for a given YJ97 engine mounting location. Three interchangeable nozzles provide thrust vectoring at 0°, -15°, and +35°; a fourth nozzle is used for 15° side thrust vectoring off the vertical position. The four fixed nozzles each have a physical throat area of 120 $in.^2$. The flange bolt pattern was selected so that the exhaust nozzles could be rotated 180° to permit preliminary static ground testing with the exhaust directed upward.

4.1 DESIGN REQUIREMENTS AND DESIGN FEATURES

The ducting and exhaust nozzles were designed to the current GE design practices and the design criteria summarized in Table VII. The ducting was designed for the maximum YJ97 cycle temperature and pressure of 1400° F and 50 psi for a 100-hour test. In addition, a safety factor of 5 was applied to all stress calculations as requested by NASA. A summary of the design features is shown in Table VIII.

4.2 MATERIAL SELECTION

A wide range of materials is available to the designer since the RALS is designed for model testing and is not required to be flight weight. The primary design emphasis was focused on a cost effective design with low cost materials and ease of fabrication of one-of-a-kind demonstrator hardware with a minimum of tooling.

AISI 321 stainless steel was selected for all low stressed components that include the transition and long extension duct. Hastelloy X was selected

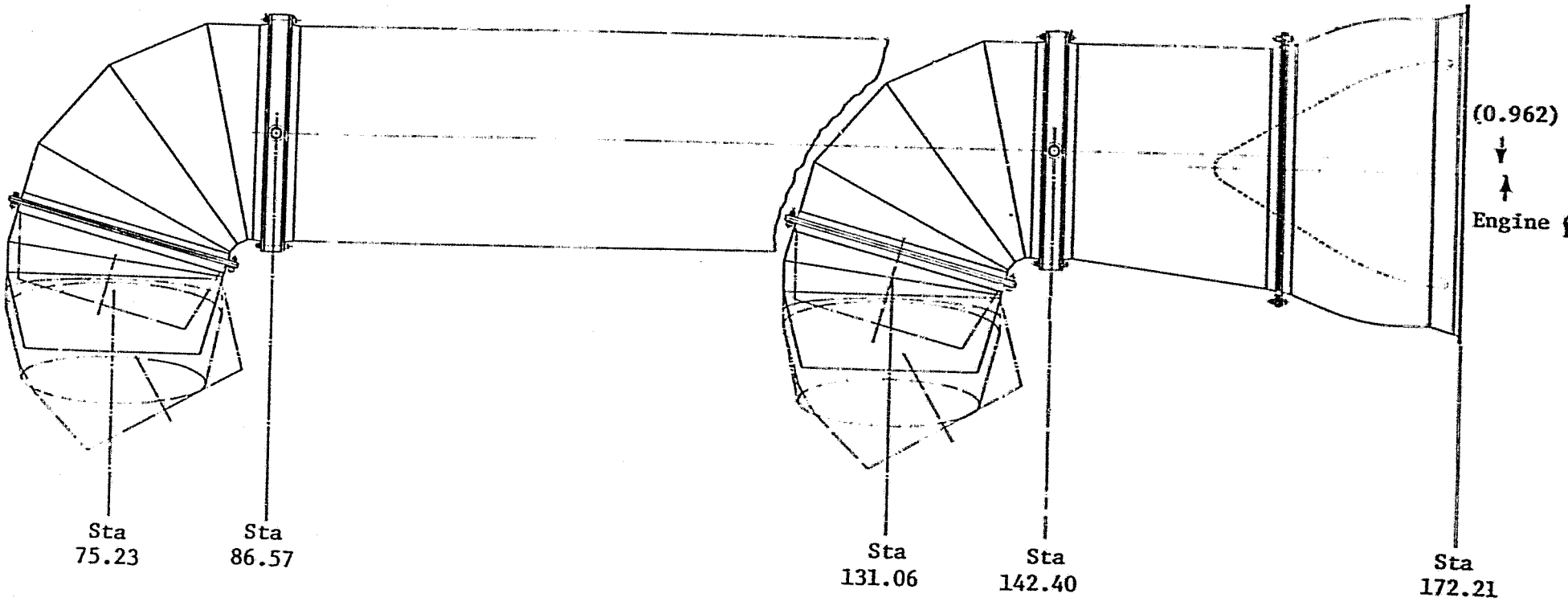

Figure 17. RALS Ducting.

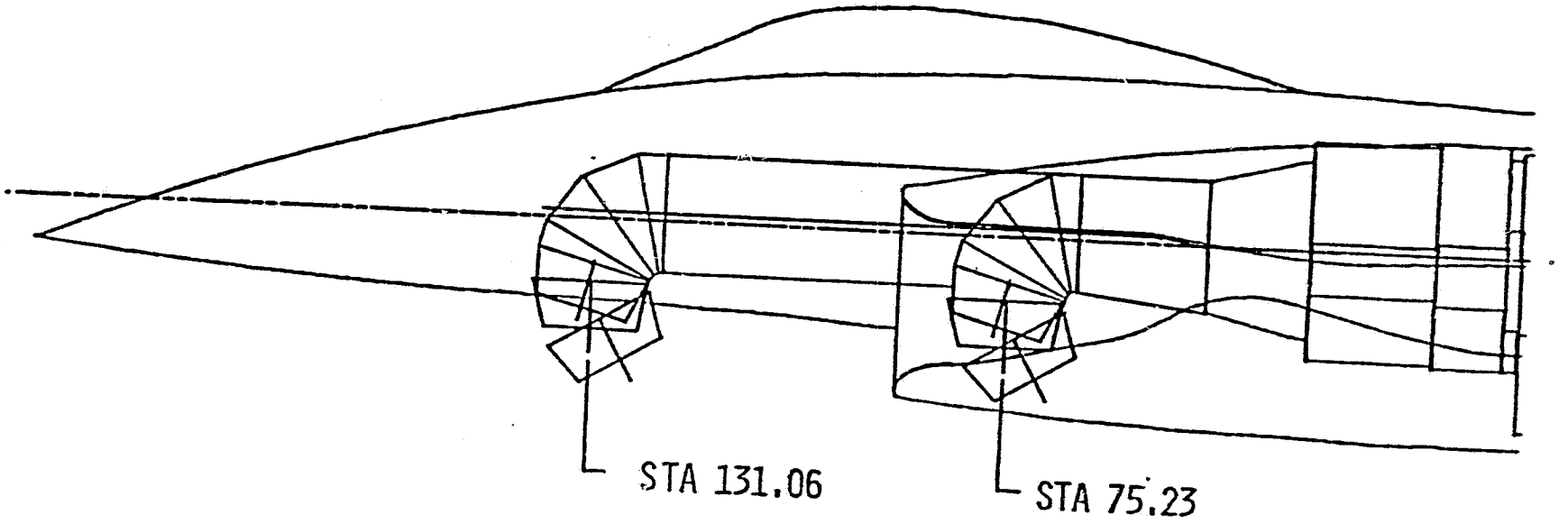

Figure 18. Exhaust Nozzle System in Aircraft Envelope.

Table VII. Exhaust System Design Criteria.

- Uncooled Duct and Exhaust Nozzle
- Nonflightweight
- 100 Hours Maximum Test Duration
- Design for Factor of Safety = 5
- Accommodate Thermal Expansion
- Duct Mount Design
- Duct Centerline Offset 0.962 inch From Engine Centerline
- Two Axial Locations of the Exhaust Nozzle
- Thrust Vector Angles
  - 15° Fwd., 0°, 30° Aft - Axial
  - ±15° Rotation From Vertical
- 120 $in.^2$ Nozzle Area

Table VIII. Exhaust System Design Features.

- Interchangeable Exhaust Nozzles
- No Seal Requirements
- Rotation of Duct in 7.5° Increments
- Mount Design Accommodates Axial Thermal Growth
- Low Cost Construction of Turning Section

for the turning duct section and all exhaust joints. These components have higher stresses at the mitered sections. If 321 stainless steel were used, thick walls would be required, which would be difficult to form and result in excessive weld distortions without expensive tooling. The mounting studs are fabricated from higher strength Inco 718 because of the high bending stress at the base of the mounts and the desirability of a reasonable diameter pin.

4.3 DESIGN DISCUSSION

The existing YJ97 exhaust diffuser duct is to be shortened by cutting off a portion of the aft conic section and welding a bolted flange to the aft end. This modification results in a lower exit stream velocity and reduced turning losses in the duct. A short spool section is added downstream of the diffuser to raise the RALS duct centerline to conform to the existing fuselage envelope. The modified diffuser and transition ducts are shown in Figure 19. A 55.83-in.-long constant area duct is inserted between the transition duct and the mount ring to move the thrust vectoring station from 75.23 to 131.06.

The 75° turning section is used in all exhaust system configurations with the appropriate nozzle to achieve the desired thrust vectoring angle as shown as Figure 20. Several methods of bend constructions were evaluated in arriving at the most cost effective solution. Die forming to provide a smooth internal flowpath would be too expensive for a one-of-a-kind demonstrator test. The mitered joint design shown in Figure 21 is typical of the manufacturing method recommended for low cost pipe bends. Sheet metal of the prescribed thickness is rolled and welded to form a cylinder to the required duct diameter. Perpendicular cuts of the cylinder are required to match the circular machined flange. Identical 12.5° angular cuts are made so that the elliptical joints of adjacent segments match. The segments are then rotated and welded together to form a mitered pipe bend of the required vectoring angle.

The longitudinal and circumferential membrane stresses in the miter bends resulting from the internal duct pressure were calculated by using the equations shown in Figure 22. The maximum stresses occur at the minimum radius of curvature (inside of the bend).

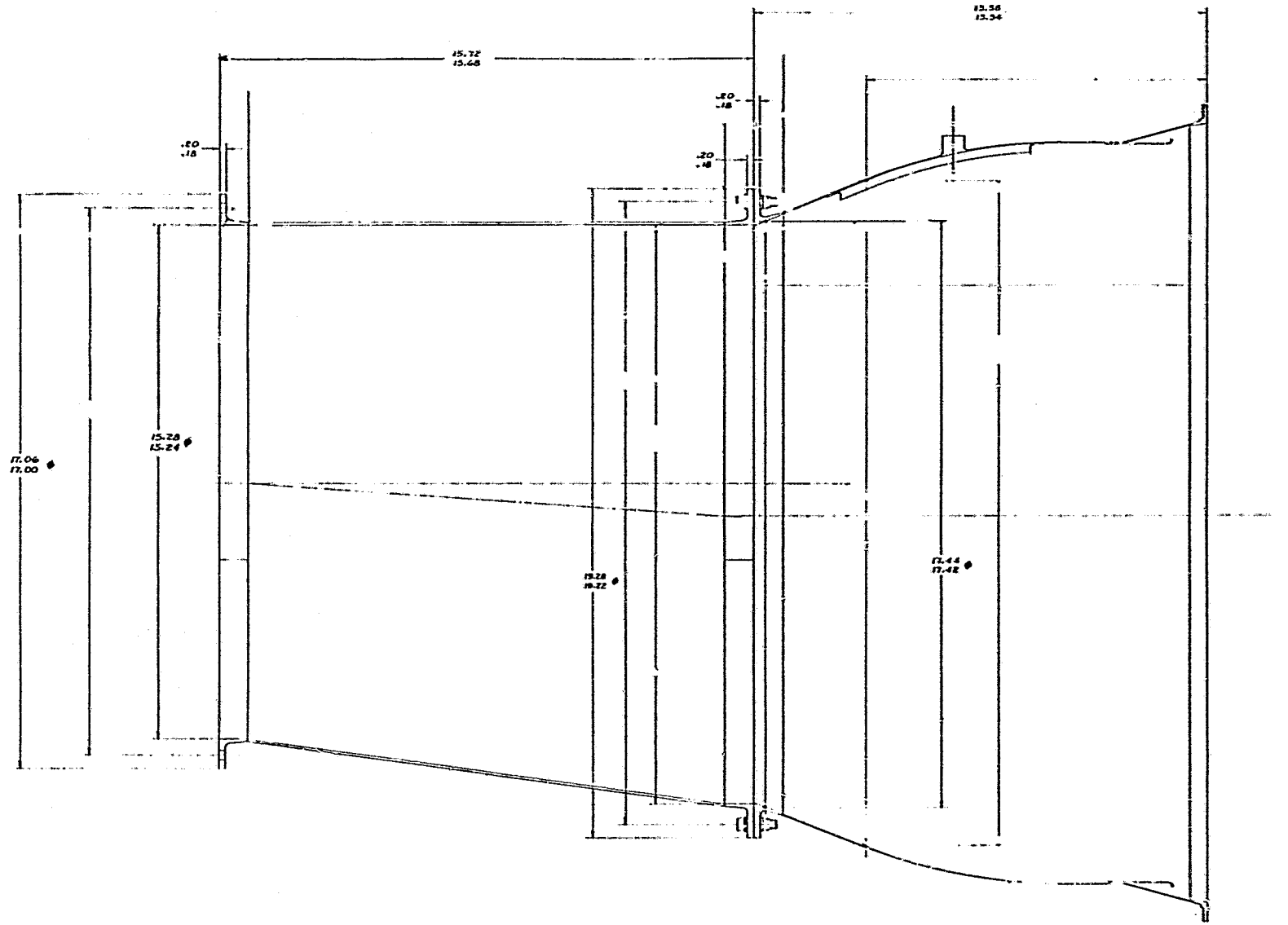

Figure 19. Exhaust Gas Diffuser and Transition Duct.

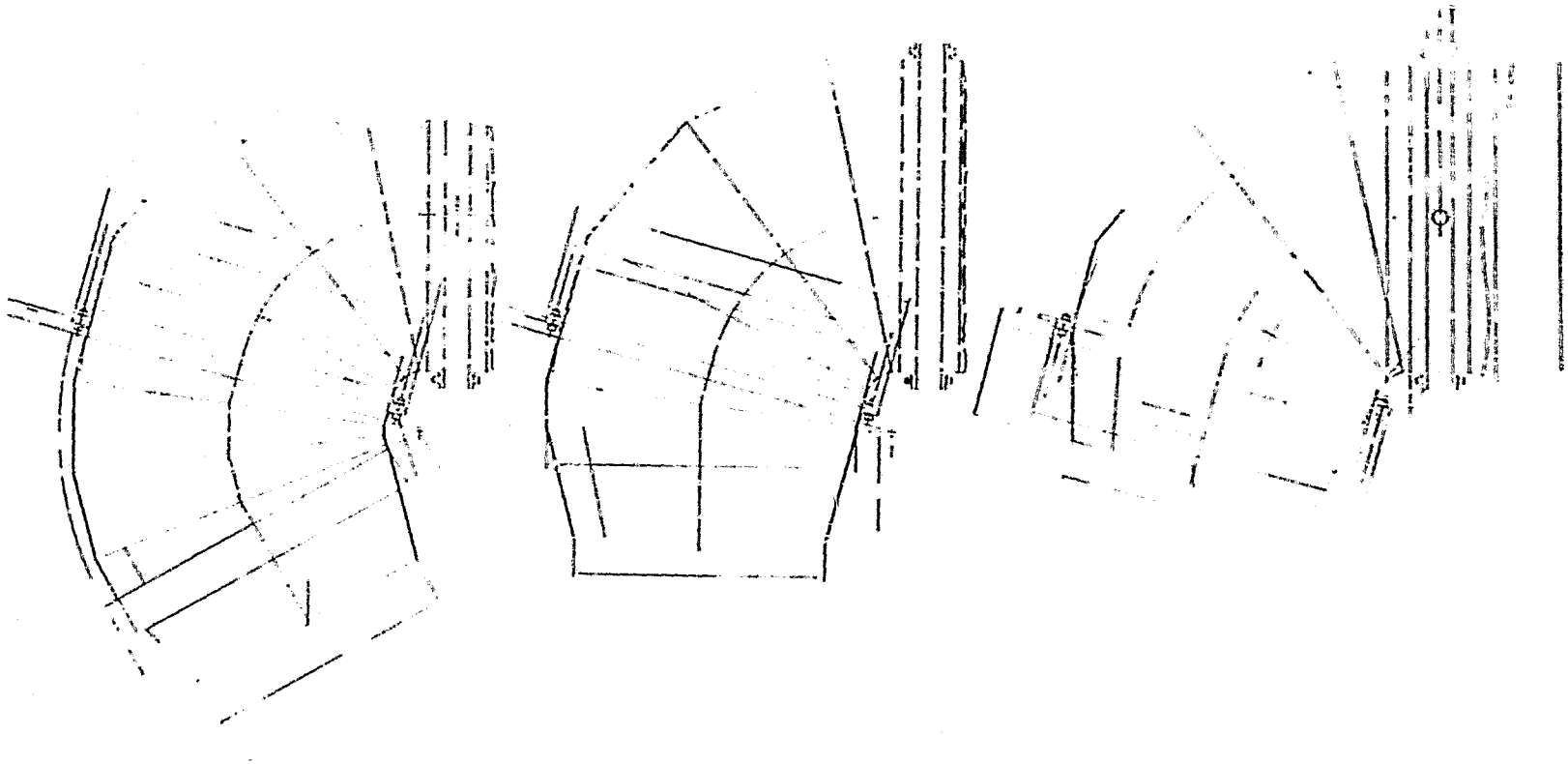

Figure 20. Turning Duct and Exhaust Nozzles.

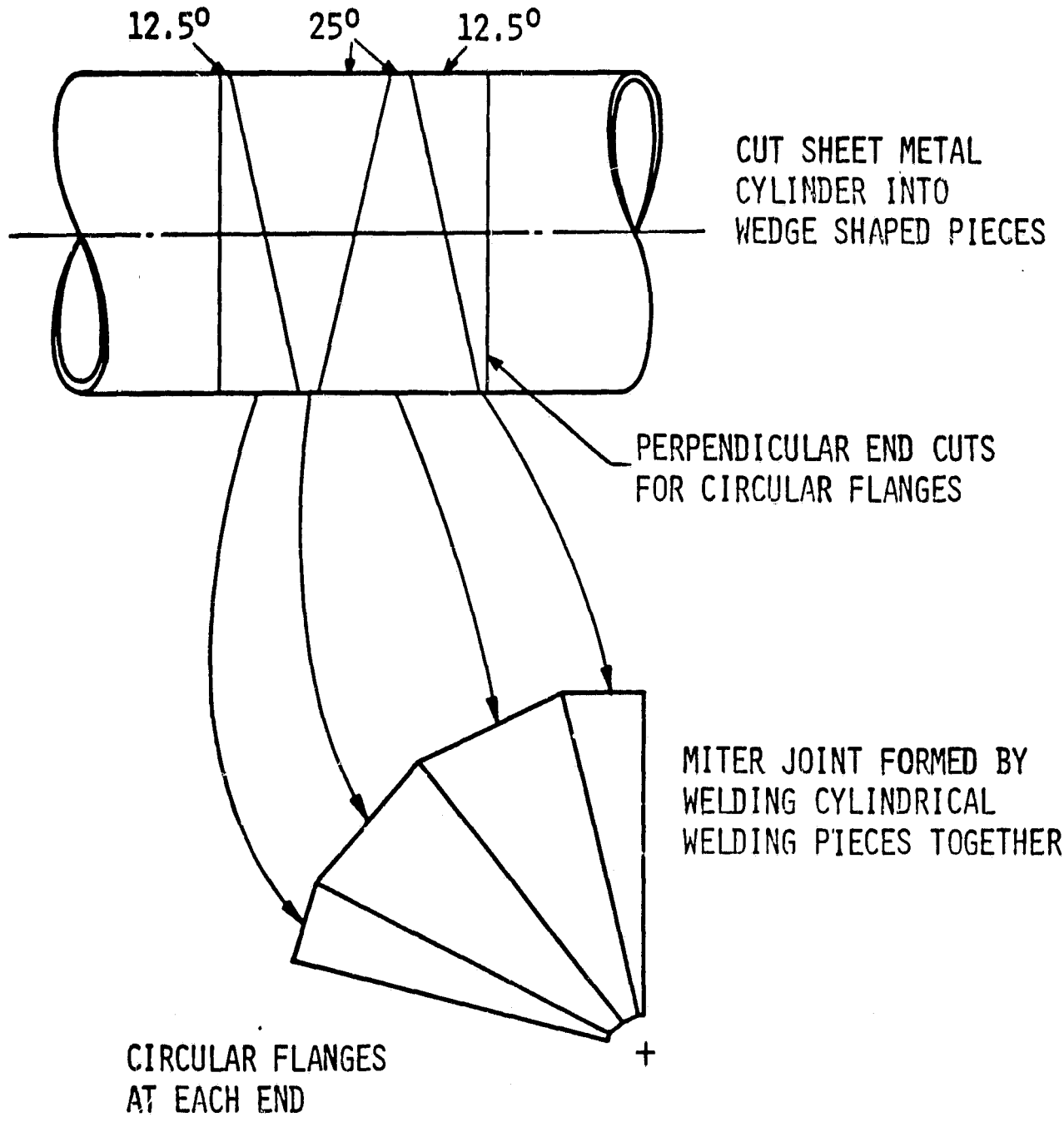

Figure 21. Turning Duct Construction.

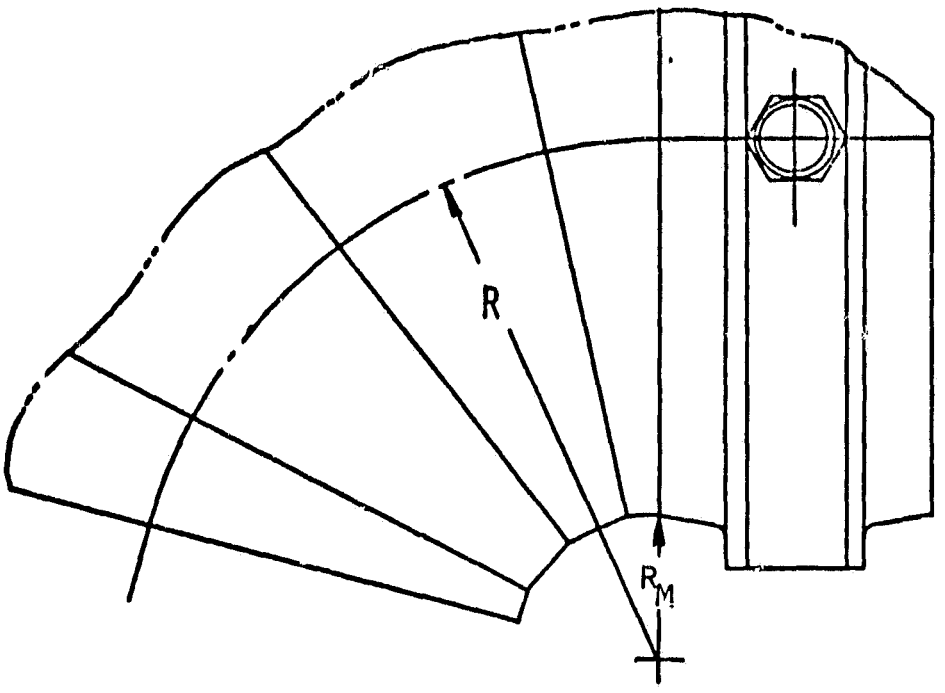

σ_L = 1.7 ksi

σ_C (MAX.) = 10.6 ksi

MATERIAL: HAST X @ 1400° F

0.12 - 0.13 in. THK.

52 ksi - TENSILE ULTIMATE

STRESSES DUE TO INTERNAL PRESSURE:

$$\sigma_L = \frac{R_M P}{2T}$$ LONGITUDINAL MEMBRANE STRESSES

$$\sigma_C = \frac{2R + R_M \sin\theta}{2(R + R_M \sin\theta)} \frac{R_M P}{T}$$ CIRCUMFERENTIAL MEMBRANE STRESSES

Figure 22. Turning Duct Internal Pressure Stresses.

The J97 engine was designed to meet very high thrust-to-weight objectives; and, therefore, it is relatively sensitive to externally applied loads. High shear or moment loads applied to the rear flange of the engine can distort the casing and cause excessive compressor blade tip rubs. A limiting safe load condition was calculated by estimating the weight and center of gravity of the straightening section and exhaust duct that were furnished with the engine. Under a 4 g maneuver condition, these parts apply a 232-lb shear load and 4432 in.-lb moment to the rear flange of the engine. To minimize these loads, the remote exhaust nozzle mounting system shown in Figure 23 was designed. The location of the mount ring was selected to minimize the bending moments transmitted to the engine by the vectored thrust loads. Details of the mounting stud are shown in Figure 24. A flange bolt is inserted through each mounting stud to prevent its rotation after assembly. A 12-in. link connecting the mounting stud to the airframe is required to minimize the vertical movement of the mounting ring due to the axial thermal growth of the hot duct. Thermal expansion of the duct at operating temperature causes the link to rotate through an angle of 6° maximum. The link end can be offset initially so that the duct is undeflected vertically at the design temperature as illustrated in Figure 25. The total thermal expansions of the exhaust system at the maximum cycle temperature of 1400° F are summarized in Figure 26. Reinforcement of the links is required to prevent lateral duct movement during 15° side thrust vectoring.

The recommended mounting system utilizes redundant load paths to transmit the vectored thrust loads to the model structure. Therefore, an accurate analysis of the shear and moment loads applied to the engine will require detailed knowledge of the stiffness of the supporting structure. It is recommended that such an analysis be conducted in the course of the model redesign to ensure that the loads on the engine do not exceed those that were calculated for the engine-furnished exhaust system.

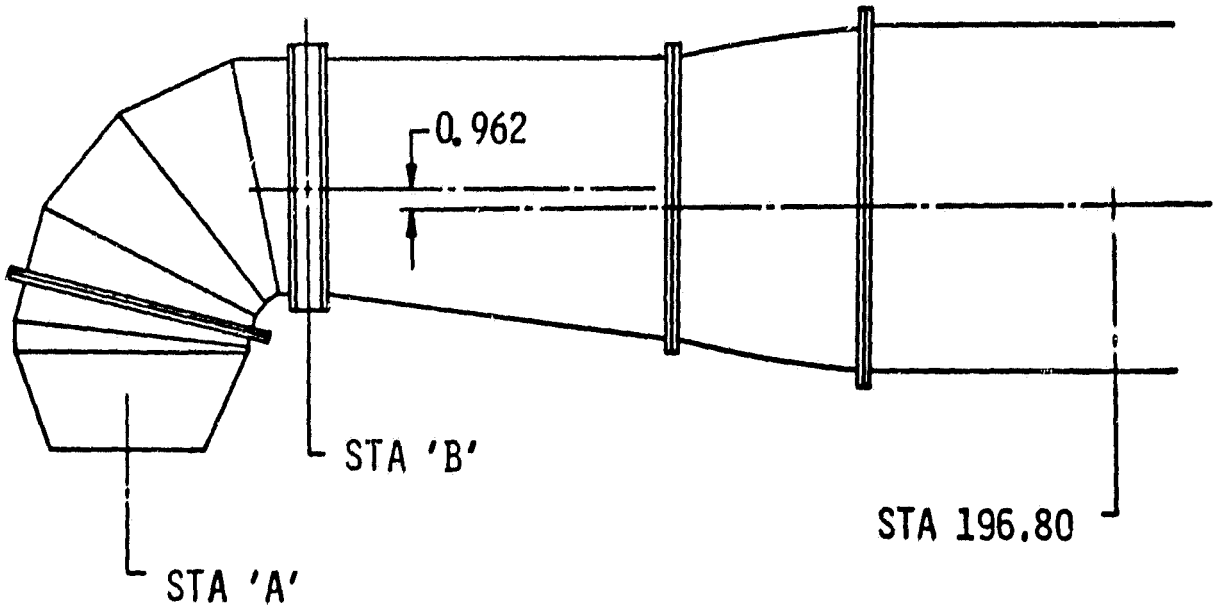

EXHAUST NOZZLE STA 'A'	DUCT MOUNT STA 'B'
131.06	142.28
75.23	86.45

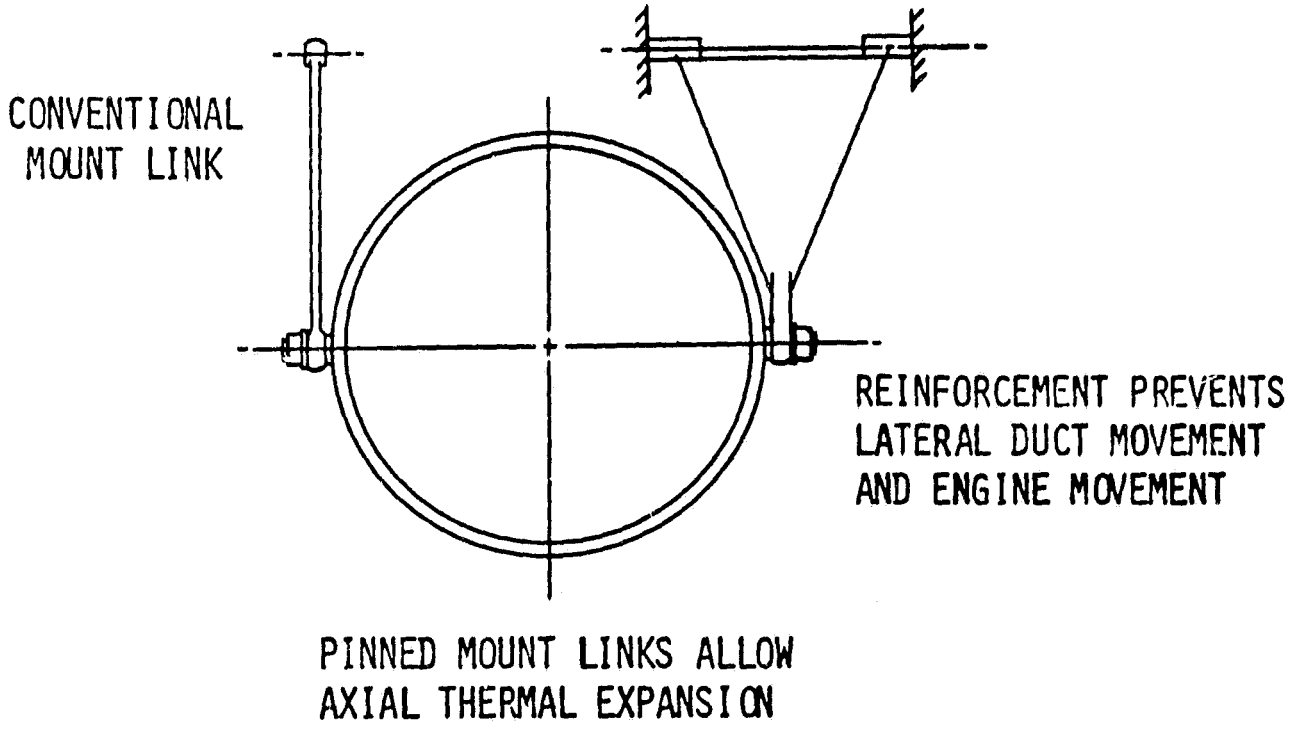

Figure 23. RALS Duct Mount.

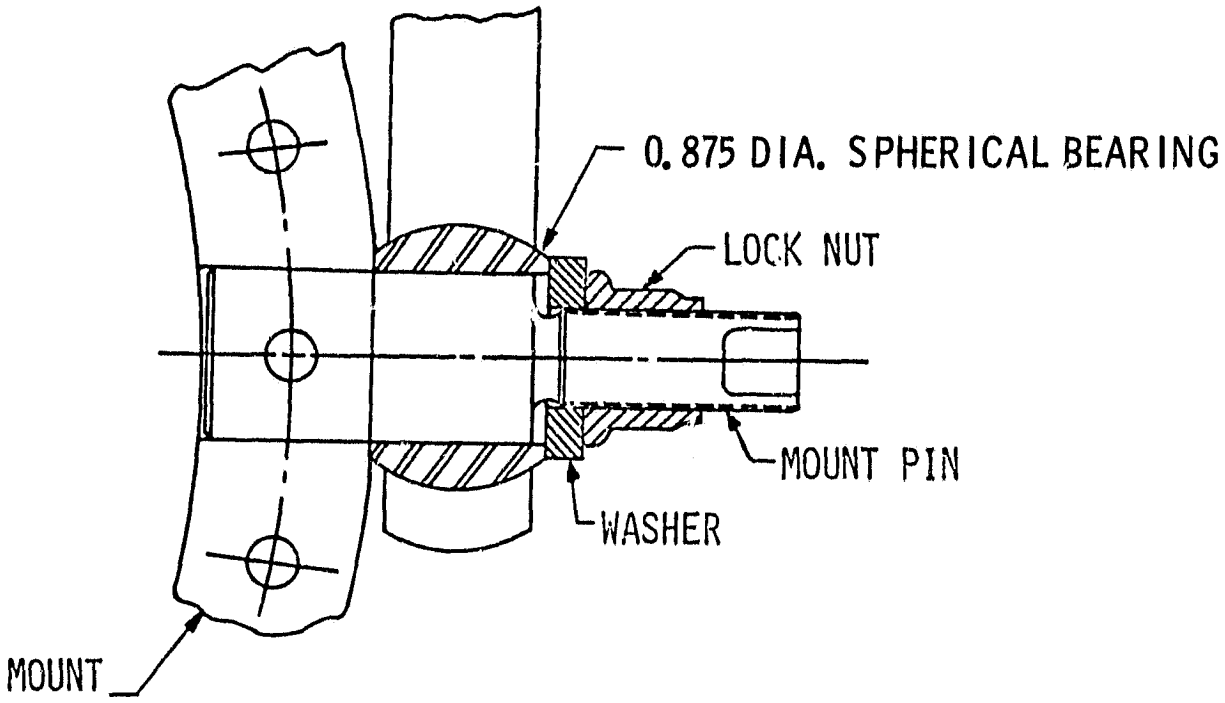

MOUNT PIN MATL: INCO 718
108 ksi (-3σ) - 0.02% Y.S.
1000° F MAX. TEMP.
σ BEND = 20.8 ksi
σ SHEAR = 5.3 ksi

FEATURES:

- ACCOMMODATES AXIAL THERMAL GROWTH
- LOCATION MINIMIZES MOMENT LOADS TO ENGINE
- FLANGE BOLT PREVENTS STUD ROTATION
- INTERCHANGEABLE WITH ALL FLANGES
- ALLOWS ROTATION OF TURNING DUCT IN 7.5° INCREMENTS WITHOUT AFFECTING AIRFRAME MOUNT HARDWARE

Figure 24. Mount Assembly Details.

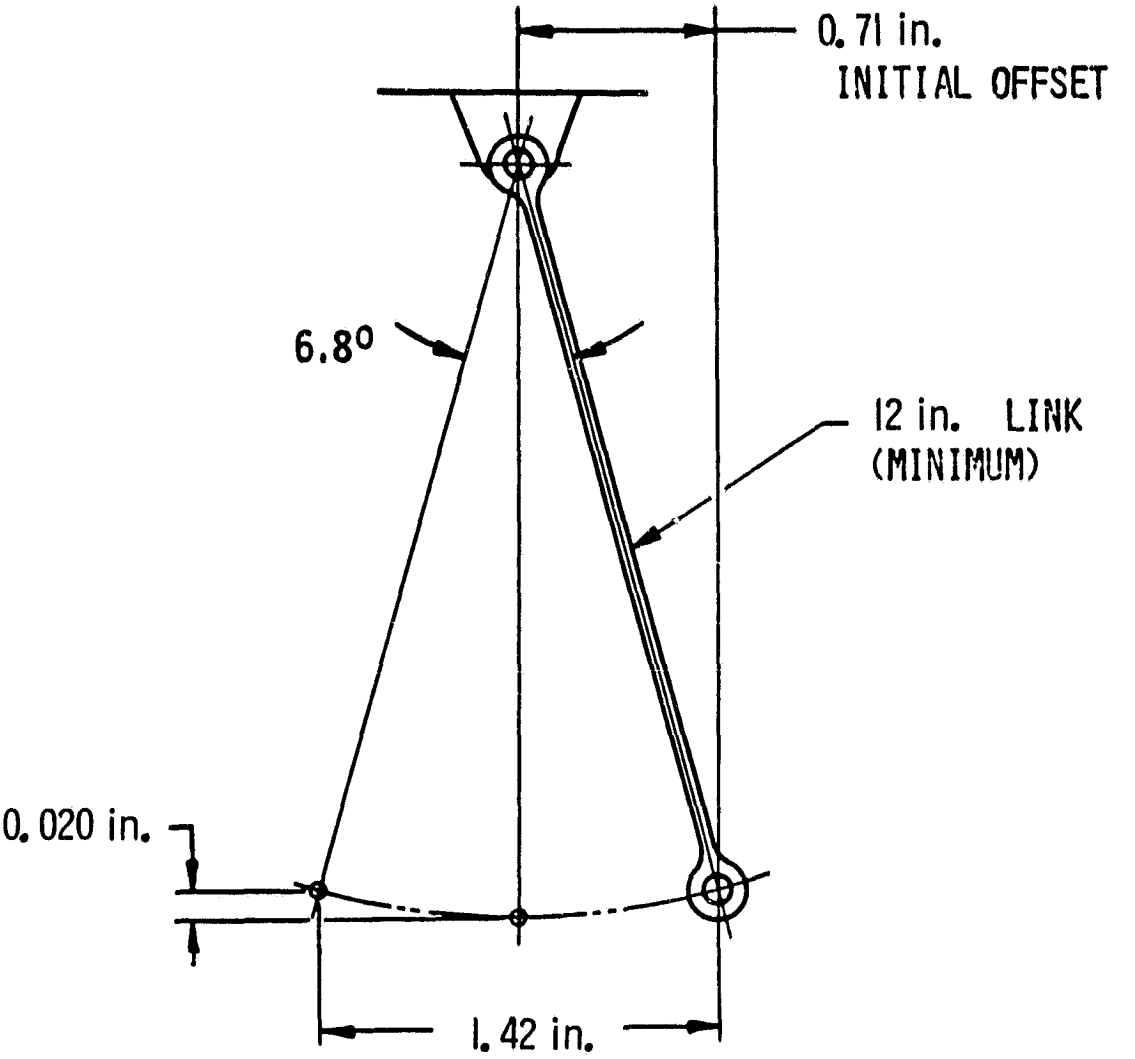

Figure 25. RALS Mount Link Deflection Owing to Duct Thermal Expansion.

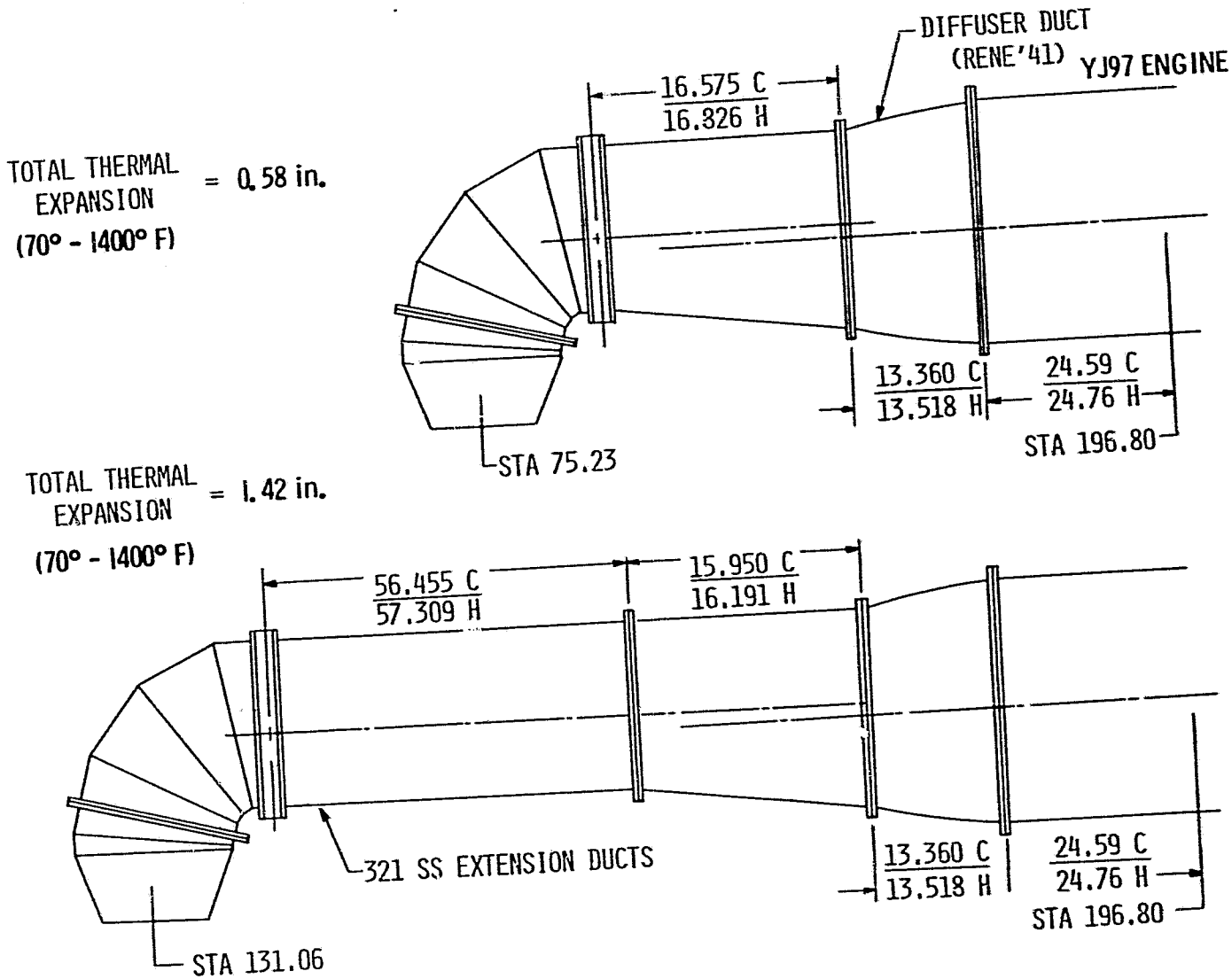

Figure 26. Exhaust System Thermal Expansion.

5.0 RESULTS AND CONCLUSIONS

This study has provided a design approach to the modification of the NASA-ARC large-scale fighter model to investigate the vertical takeoff and landing flight modes. The model is typical of a number of proposed designs with respect to the general arrangement of vectorable exhaust nozzles, inlets, pilot compartment, and other features. By adding a third J97 engine mounted in the fuselage, hot gas can be supplied to a remote vertical exhaust nozzle. This nozzle can be located near the pilot's compartment to simulate the forward exhaust nozzle of a RALS system. Operating in a hover test facility or in a wind tunnel can provide valuable data and insight into the operating characteristics of a V/STOL fighter.

Among the characteristics that can be investigated and for which an inadequate data base currently exists are:

- Reingestion limits at various angles-of-attack and wind angles
- Suckdown and fountain effects on the aircraft and inlet flow field
- Deck heating problems
- The use of combinations of thrust vectoring and throttle response to control aircraft attitude
- Control requirements in the transition flight regime with partially effective aerodynamic control surfaces.

In addition, the modified model will provide a realistic test vehicle for other new V/STOL propulsion concepts. For example, should a useful ejector nozzle concept result from NASA-Lewis Contract NAS3-22042, this concept could be verified using the large-scale model.

This study has provided a layout for the vehicle that achieves a number of desired characteristics:

- Inlets are located at the front of the nacelles to produce realistic aerodynamic moments on the vehicle.
- Alternate inlets in the top of the nacelles may be used in the vertical operating mode to simulate auxiliary inlets that are shielded from reingestion.

- Although the inlet ducts to the third engine are relatively long and complex, they can be housed in the wing root with an acceptable external aerodynamic contour.

- Because of the complex three-dimensional flow field of the inlet systems, accurate ram recovery levels cannot be determined. However, the use of moderate duct Mach number will hold pressure losses to acceptable levels. In addition, the use of an inlet plenum, turning vanes, and an inlet screen will adequately control inlet pressure distortion.

- An inlet compatibility analysis was conducted, indicating that the J97 engine will operate without compressor stall. Results of this analysis include recommendations as to operational procedures and the use of inlet-instrumentation to ensure stall-free operation.

- An exhaust system detail design was completed to simulate a RALS nozzle. Two axial positions of the nozzle can be investigated by using a spool-piece in the ducting. All ducting has been designed using conventional materials and manufacturing methods to produce nonflightweight test hardware.

As a result of this study, sufficient design information has been generated to ensure that there are no mechanical or aerodynamic limitations that will interfere with the intended use of the model. Since the RALS concept remains a viable alternate for both V/STOL and STOL fighter aircraft, it is recommended that the large-scale STOL model be modified and tested to provide the needed data base.

Table IX. LIST OF SYMBOLS, ACRONYMS AND CONVERSIONS.

SYMBOLS

A	Area
A_{e8}	Exhaust Nozzle Throat Effective Area
A8	Exhaust Nozzle Throat Area
A9	Exhaust Nozzle Exit Area
C_F	Flow Coefficient
C_V	Exhaust Nozzle Velocity Coefficient
F_N	Thrust
K_P	Pressure Distortion
K_T	Temperature Distortion
OPR	Overall Pressure Ratio
P	Total Pressure
P/P	Pressure Ratio
P_s	Specific Excess Energy for Aircraft Maneuverability
P_{2C}	Compressor Inlet Total Pressure
P_3	Compressor Discharge Total Pressure
P_8/P_o	Nozzle Expansion Ratio
RSS	Root Sum Square
R_{Duct}	Duct Radius
R_{INT}	Internal Bend Radius
SM_A	Surge Margin Available
T	Total Temperature
T_{EXH}	Exhaust Gas Temperature
T_{41}	Turbine Rotor Inlet Temperature
V	Velocity
WT	Weight
W_a	Airflow
ΔPRS_A	Surge Pressure Ratio Loss Available
ΔPRS_D	Net Pressure Ratio Margin
ΔPRS_I	Internal Surge Pressure Ratio Loss

Table IX. LIST OF SYMBOLS, ACRONYMS AND CONVERSIONS (Continued).

SYMBOLS (Concluded)

η_C	Compressor Adiabatic Efficiency
η_R	Ram Recovery
σ_C	Circumferential Stress
σ_L	Longitudinal Stress

ACRONYMS

ARC	Ames Research Center
ARP	Aerospace Recommended Practice
FOD	Foreign Object Damage
IAGS	Interactive Graphics System
NASA	National Aeronautics and Space Administration
RALS	Remote Augmented Lift System
SAE	Society of Automotive Engineers
STOL	Short Takeoff and Landing
SWB	Spanwise Blowing
TOGW	Takeoff Gross Weight
USAF	United States Air Force
US/FRG	United States/Federal Republic of Germany
V/STSOL	Vertical/Short Takeoff and Landing
VTOL	Vertical Takeoff and Landing

CONVERSIONS

English to Standard International Units

Mass	lb x 0.4536 = kg
Force	lb x 4.448 = N
Distance	ft x 0.3048 = m
Distance	nmi x 1.852 = km
Distance	in. x 2.54 = cm
Area	ft^2 x 0.929 = m^2
Area	$in.^2$ x 6.4516 = cm^2
Area	Acres x 0.04047 = km^2

Table IX. LIST OF SYMBOLS, ACRONYMS AND CONVERSIONS (Concluded).
English to Standard International Units (Concluded)

Volume	$in.^3 \times 16.387 = cm^3$
Volume	$ft^3 \times 0.0283 = m^3$
Volume	$gal \times 0.003785 = m^3$
Velocity	$ft/sec \times 0.3048 = m/sec$
Velocity	$knots \times 0.51444 = m/sec$
Power	$hp \times 745.7 = W$
Temperature	$(° F + 460) \times 5/9 = ° K$
Heat	$Btu \times 1055.9 = J$
Airflow	$lb/sec \times 0.4536 = kg/sec$
Thrust	$lb \times 4.448 = N$
sfc	$lb/hr/lb \times 0.0283 = g/sN$
F_N/W_t	$lb/lb \times 9.806 = N/kg$
F_N/W_a	$lb/sec/lb \times 9.806 = Ns/kg$
Wt/Area	$lb/ft^2 \times 4.877 = kg/m^2$
Heat Load	$Btu/lb \times 2327.8 = J/kg$
Pressure or Stress	$psia \times 0.6895 = N/cm^2$
Torque	$in.-lb \times 11.3 = cm\ N$
Torque	$ft-lb \times 1.356 = m\ N$
Vol. Flow	$gpm \times 63.0 = cm^3/sec$
Heat Flow	$Btu/min \times 17.6 = J/sec$
Unit Load	$lb/in. \times 1.75 = N/cm$
Density	$lb/ft^3 \times 16.028 = kg/m^3$

REFERENCES

1. "Variable Cycle Engine Evaluation for Supersonic V/STOL Fighter Final Summary Report," General Electric Company, R78AEG599.

2. "Variable Cycle Engine Evaluation for Supersonic V/STOL Fighters," McDonnell Douglas Corporation, N00140-75-C-0034.

3. "Study of Aerodynamic Technology for V/STOL Fighter/Attack Aircraft - Phase I Final Report," Grumman Aerospace Corporation, NASA CR-152129.

4. "Remote Augmentor Lift System/Variable Cycle Engine Trade Study - Final Report," General Electric Company, R80AEG455.

5. "US/FRG V/STOL Vectored Thrust Cruise Propulsion System Design Report," General Electric Company, Contract No. F33657-67-C-1401, p 67-85.